Am J Cancer Res 2020;10(12):4287-4307
www.ajcr.us /ISSN:2156-6976/ajcr0120106

Original Article

Inhibition of caspase-3-mediated GSDME-derived pyroptosis aids in noncancerous tissue protection of squamous cell carcinoma patients during cisplatin-based chemotherapy

Zixian Huang[1,2*], Qianyu Zhang[1,2*], Yan Wang[1*], Rui Chen[1], Yongqiang Wang[2], Zhuoshan Huang[1,2], Guangming Zhou[1,2], Haigang Li[3], Xi Rui[1,2], Tingting Jin[1], Shihao Li[1,2], Yin Zhang[2], Zhiquan Huang[1]

[1]Department of Oral and Maxillofacial Surgery, Sun Yat-sen Memorial Hospital, Sun Yat-sen University, Guangzhou, Guangdong, China; [2]Guangdong Provincial Key Laboratory of Malignant Tumor Epigenetics and Gene Regulation, Sun Yat-sen Memorial Hospital, Sun Yat-sen University, Guangzhou, China; [3]Department of Pathology, Sun Yat-sen Memorial Hospital, Sun Yat-sen University, Guangzhou, Guangdong, China. [*]Equal contributors and co-first authors.

Received August 11, 2020; Accepted October 13, 2020; Epub December 1, 2020; Published December 15, 2020

Abstract: The side effects of platinum-based chemotherapy are important factors limiting the survival of oral squamous cell carcinoma (OSCC) patients. Current research suggests that pyroptosis is involved in this process. However, how this mechanism can be used to reduce side effects has not yet been elucidated. In this study, we reported that GSDME was expressed at higher levels in normal tissues than in cancerous tissues in OSCC patients and was the main cause of platinum-based side effects. In an OSCC xenograft model, the inflammatory status and GSDME expression were increased after cisplatin chemotherapy. Cellular experiments showed that higher expression of GSDME was associated with less chemoresistance to cisplatin. A subsequent study demonstrated that cisplatin treatment promotes the maturation of caspase-3, triggers GSDME-mediated pyroptosis and induces cell death. When the amino acid sequence of GSDME cleaved by caspase-3 was mutated, cellular death and pyroptosis induced by cisplatin were significantly inhibited. Moreover, application of vitamin D during cisplatin-based chemotherapy could successfully inhibit GSDME cleavage and pyroptotic cell death *in vitro* and *in vivo*. Taken together, our study revealed that vitamin D can inhibit caspase-3-mediated GSDME cleavage and thus reduce normal tissue pyroptosis, relieving chemotherapeutic side effects. Inhibition of systemic GSDME during chemotherapy is currently unachievable. Vitamin D supplementation during chemotherapy in OSCC patients might be able to reduce the process described above and benefit patients. However, additional follow-up clinical studies are needed.

Keywords: Gasdermin E, pyroptosis, chemotherapy side effect prevention, chemotolerance, vitamin D

Introduction

Oral cancer accounts for 2.9% of all malignant tumours worldwide [1, 2] and consists mostly of oral squamous cell carcinoma (OSCC). In China, there are 48,100 new cases of oral cancer and 22,100 deaths each year [3]. Platinum-based chemotherapy, which can damage the structure of the cell membrane and cause DNA damage with tumour-specific sensitivity, is an important part of oral cancer treatment. The 5-year survival rate of patients who receive cisplatin chemotherapy is 10-20% higher than that of patients who receive surgery alone [4, 5]. However, the reported side effects from platinum-based drugs cannot be ignored [6]. Nephrotoxicity, digestive tract reactions, oral mucosal inflammation and ulceration caused by platinum-based drugs seriously affect follow-up treatment and prognosis [7, 8].

The epithelial secretions and histopathological examination of mucositis caused by cisplatin chemotherapy revealed increased TNF-α, IL-1β and NF-κB [9]. The secretion of TNF-α, IL-1β and IL-18 into the gastrointestinal mucosa was also increased [10]. These reports suggest that the side effects of platinum-based drugs may be

associated with pyroptosis, which is a pattern of inflammatory-related programmed cell death [11]. It is characterized by inflammatory stimulation, cell membrane perforation, and the release of mature IL-1β [12]. Hence, pyroptosis might be involved in the side effects of cisplatin chemotherapy.

Currently, exploring effective ways to inhibit pyroptosis is important for the prevention and treatment of side effects from platinum-based chemotherapy. In this study, we observed the inflammatory response induced by cisplatin in normal tissues of OSCC xenograft models. Cisplatin subsequently stimulated gasdermin family protein E (GSDME) expression, which was also highly expressed in adjacent noncancerous (ANC) tissues compared with cancerous tissues in OSCC patients. As mature caspase-3 was also induced by cisplatin, GSDME was cleaved and induced pyroptosis; thus, the associated side effects were subsequently observed. As cleavage was inhibited, cellular cisplatin chemoresistance enhanced. Based on the above mechanism, the application of vitamin D during chemotherapy could inhibit GSDME-mediated pyroptosis by inhibiting caspase-3-GSDME cleavage and relieve cisplatin-induced side effects *in vivo* and vitro. This research provides a new strategy for side effect prevention during OSCC chemotherapy.

Materials and methods

Antibodies

Antibody against FLAG was purchased from Sigma (F3165). Antibodies against caspase-1 (#3866), caspase-3 (#9662, cleaved #9664), NLRC4 (#12421), and GAPDH (#D16H11) were purchased from Cell Signaling Technology. NAIP (#ab25968) was purchased from Abcam. GSDMD (#sc-81868), goat anti-mouse IgG-HRP (sc-2005) and goat anti-rabbit IgG-HRP (sc-2004) were purchased from Santa Cruz Biotechnology. GSDME (#ab215191) was purchased from Abcam.

Reagents

The vitamin D metabolite 1,25D3 (#17936) and vitamin C (L-Ascorbic acid, #A4403) were purchased from Sigma (USA). Aspirin (#SA8970), celecoxib (#IC0230), and hydrocortisone (#IH-0100) were purchased from Solarbio (Beijing, China). The reagents described above were dissolved in anhydrous alcohol (AA) at concentrations according to the manufacturer's instructions for preservation. Immediately prior to use, the stock solution was diluted to the indicated concentrations in culture medium. Specifically, vitamin D were dissolved into 30 μM as stock, and diluted to a final concentration of 30 nM in culture medium.

Other chemicals were purchased from Sigma. All culture media and foetal bovine serum (FBS) were purchased from Bioind.

Plasmids

The cDNAs encoding human GSDME (NM_001127453, wild type) were synthesized by Vigene Biosciences (Shandong, China); mutants of GSDME with "ATAGACATGCCAGATGCT" transformed into "GGTGGAAGTGGTGGAAGT" were generated by IGE Biosciences (Guangzhou, China).

For stable expression in cell lines, GSDME cDNA was inserted into a modified pCDH lentiviral vector with an N-terminal Flag-tag.

Human GSDME short hairpin RNAs (shRNAs) were purchased from Vigene Biosciences, and the sequence of the shRNA was as follows: "GGATGGACCATTAAGTGTTTTCAAGAGAAACACTTAATGGTCCATCCTTTTTT".

The px458 plasmid used for generating the GSDME knockout cells was obtained from IGE Biosciences (Guangzhou, China). The sgRNA sequences were as follows: "caccCAGTTTTTATCCCTCACCCTgttt".

pMD2.G (#12259, Addgene) and psPAX2 (#12260, Addgene) were used as packaging vectors.

All the constructs were confirmed by both DNA sequencing and diagnostic digestion.

Cell culture and transfection

Human umbilical vein endothelial cells (HUVECs), gastric squamous epithelial cells (GSEs), OSCC (CAL-27 & SCC-9) cells, and HEK293 cells were obtained from the American Type Culture Collection (ATCC). Normal oral squamous epithelial cells (NOKs) were purchased from Cell Bank of the Chinese Academy of

Sciences (Shanghai, China). All cell lines were routinely cultured in DMEM or DMEM-F12 medium supplemented with 10% FBS in a 37°C humidified incubator containing 5% CO_2. All the cell lines were validated by short tandem repeat profiling analysis and were free of mycoplasma contamination.

Transient transfection of cells was performed using Lipofectamine 3000 (Invitrogen) reagent according to the manufacturer's instructions.

For stable expression, lentiviral plasmids harbouring the desired gene were first transfected into 293T cells together with the pSPAX2 and pMD2.G packaging plasmids at a ratio of 5:3:2. HEK293 cells were placed in a 10-cm plate and cultured as previously described. After reaching 70-80% confluence, the cells were transfected with 6 μg of psPAX2, 4 μg of pMD2.G and 10 μg of transfer vector using Lipofectamine 3000 reagent. At 48 hours after transfection, the supernatants of each group were collected and used to infect the indicated cells for another 48 hours. Puromycin-tolerant cells were selected. Subsequent Western blotting and PCR analyses were applied to confirm the correct expression of the stable cell lines.

For GSDME knockout, CRISPR plasmid PX458 containing GSDME sgRNA was transfected into indicated cell lines using Lipofectamine 3000 at 70% confluency. At 48 hours after transfection, the cells with green fluorescence were selected by flow sorting, and the function of sgRNA was confirmed by Western blot and Sanger sequencing of genome DNA.

Western blot analysis

For protein extraction, the cells were washed twice with cooled phosphate-buffered saline (PBS), harvested by scraping and then lysed in lysis buffer (#9803, CST). Following centrifugation, the supernatant was collected, and the protein concentration was determined using the BCA Protein Assay Kit (#23227, Thermo Scientific).

For Western blotting, cell lysates were electrophoretically separated on an SDS-PAGE gel using a standard protocol. The proteins were then transferred to Immobilon-P transfer membranes (PVDFs) (IPVH00010; Millipore, USA). The membranes were blocked with 5% non-fat milk in Tris-buffered saline containing 0.1% Tween-20 (TBST) for 1 hour at room temperature. The blots were incubated with the antibodies mentioned above at 4°C overnight, washed in TBST and then probed with the appropriate secondary antibody. Western blot analysis was performed according to standard protocols.

RNA extraction and real-time quantitative RT-PCR

Total RNA was extracted using TRIzol reagent (Takara, Japan) according to the manufacturer's instructions and then reverse transcribed into cDNA using PrimeScript™ RT Master Mix (Takara, Japan) on an ABI 9700 Real-Time PCR system (ABI, USA). The newly synthesized cDNA was then used as a template to detect the desired genes.

Specifically, 1 μl of cDNA was mixed with TB Green® Premix Ex Taq™ II (Takara, Japan) in a 20-μl reaction volume. All the reactions were run in triplicate using the primers described above. The reaction conditions were as follows: 94°C for 2 minutes, 94°C for 20 s, 58°C for 20 s and 72°C for 20 s for 40 cycles. Relative mRNA expression was detected using a Roche LightCycler 480 II Real-time PCR machine (Roche, USA). The primer sequences were listed in **Table 5**:

Table 5. Primer Sequences used for PCR

Gene	Forward Primer	Reverse Primer
GSDME	TGCCTACGGTGTCATTGAGTT	TCTGGCATGTCTATGAATGCAAA
GSDMD	GGACAGGCAAAGATCGCAG	CACTCAGCGAGTACACATTCATT
GAPDH	GAGTCAACGGATTTGGTCGT	GACAAGCTTCCCGTTCTCAG

DNA isolation and genomic sequencing

Genomic DNA was isolated from stable cell lines using a DNA isolation kit (#3101050, Simgen, China). Then, the genomic DNA sequence of the GSDME and GSDME mutant in stable cell lines was analysed using the following primers: Forward "ATTTAATTGCTGGTGTGAGACCTTCCAAAA"; Reverse "AGGCCTGACGTGACACATTATAGCTTAACC". Sequences were then analysed using the forward primer.

Flow cytometry (FCM)

For the flow cytometric quantification of cell death, the cells were treated as indicated. Then, the cells were collected, washed twice

with PBS and stained using annexin V-FITC/PI (#556547, BD) and annexin V-APC/7-AAD (#640930, Biolegend) according to the manufacturer's instructions. Stained cells were analysed using a Becton Dickinson FACScan Flow Cytometer (FACScan, BD), and data were processed using FlowJo software.

Cytotoxicity assay

Relevant cells were plated in 96-well plates (4000 cells/well) and cultured for 24 hours before treatment. Then, cell death was measured at the indicated time points with the LDH assay using a CytoTox 96 Non-Radioactive Cytotoxicity Assay Kit (#G1781, Promega) according to the manufacturer's protocol.

The LDH release rates were determined following the protocol of the Cell-Mediated Cytotoxicity Assay kit:

$$\%\text{Cytotoxicity} = \frac{\text{Experimental} - \text{Effector Spontaneous} - \text{Target Spontaneous}}{\text{Target Maximum} - \text{Target Spontaneous}} \times 100$$

Cisplatin cytotoxicity assay

Relevant cells were plated in 96-well plates (10,000 cells/well) and cultured for 24 hours before treatment. Then, the cells were treated with various concentrations (0, 2.5, 5, 10, 20, 40, 80, 160 and 320 μmol/L) of cisplatin (#1134357, Sigma, USA), and the MTS assay (#G358C, Promega) was applied to examine the cytotoxicity of cisplatin after 48 hours of treatment. The medium was removed from each well, and 100 μl of a mixture of 10% MTS in DMEM was added. The plates were incubated for an additional 2 hours and measured at an absorbance of 490 nm using a microplate reader (Multiskan MK3, China).

The relative cell survival (%) was determined by the formula (OD × χ μmol/L/OD 0 μmol/L) × 100, where χ represents the cisplatin concentration.

The percentage of cell mortality (%) was then calculated as 100 - relative cell survival.

ELISA

Relevant cells were plated in 96-well plates (5000 cells/well). After an overnight incubation, the cells were treated with cisplatin or vitamin D at the indicated concentrations for an additional 24 hours. The supernatant was collected to detect IL-1β and TNF-α secretion using ELISA Kits (IL-1β, # ab27059, TNF-α, # ab27001 ABsci; vitamin D, # TL-E1339, Telenbiotech).

Microscopy imaging

To examine cisplatin cytotoxicity and the morphology of apoptotic and pyroptotic cells, cells were plated in a 96-well plate (#3599, Costar Corning) and cultured overnight. Cells were observed and captured using high-content microscope imaging observation (iBright CL1000, ImageXpress Micro Confocal). To record the cell death process, the indicated cells were seeded at approximately 40-50% confluency. Then, the cells were treated with cisplatin, and videos were obtained under bright light microscopy. Live cell imaging was conducted in an Okolab cage enclosure with temperature (37°C) and environmental (5% CO_2, humidity) controls. Images were obtained every 10 minutes for 24 hours. All imaging data shown are representative of at least three randomly selected fields. The images were processed using the ImageJ program.

OSCC sample collection and patient follow-up

To address the research purpose, patients presenting at the Department of Oral and Maxillofacial Surgery at Sun Yat-sen Memorial Hospital between 2011 and 2013 for the treatment of OSCC were recruited. Inclusion criteria included a pathological diagnosis of OSCC, a need to undergo cisplatin chemotherapy, and a willingness to participate in the subsequent follow-up. Patients were excluded as study subjects if they were diagnosed with multiple cancers or other severe diseases. Data on the features of the OSCC patients, including age, sex, tumour differentiation, lymphatic metastasis and clinical stage, as well as the serum vitamin D concentration, were collected. All patients had a referral visit at least every season. In addition, their tumour samples and ANC samples were collected. ANC tissue refers to an area at least 2 cm from the tumour lesion representing the resection border that was pathologically confirmed as noncancerous tissue.

In vivo tumour xenograft model

To explore the effects of cisplatin and vitamin D on normal tissues during chemotherapy *in vivo*,

an OSCC xenograft (CAL-27 cells) model was first generated [13]. OSCC cells (2.0×10^6) were implanted into the right upper backs of BALB/c nude mice. When the tumour volume reached approximately 60 mm^3 (5 mm × 5 mm, length × width), 30 μg/kg of 1,25D3 or 5 mg/kg of cisplatin was intraperitoneally injected according to the treatment group. Cisplatin was administered every 4 days, and vitamin D was administered every 2 days. Normal saline (N.S.) was used as a control. The tumours were measured each time to determine the tumour volume (mm^3), which was calculated as length × $width^2 \times 0.5$. The weight of the mice was recorded simultaneously. The mice were sacrificed 2 days after the fifth injection, and the tumours, tongue, kidneys, and intestine, among other samples, were harvested, followed by paraffin embedding for immunohistochemistry (IHC).

IHC

IHC staining was performed according to standard protocols. After deparaffinization, antigen retrieval was conducted using 10 mM sodium citrate buffer (pH 8.0) in a pressure cooker at full power for 5 minutes. Briefly, the tissue sections were blocked sequentially with 3% H_2O_2 and normal serum and then incubated with the indicated primary antibodies at 4°C overnight. The tissue sections were incubated with a biotinylated secondary antibody conjugated to a streptavidin-HRP complex (ready-to-use SP kit; Zhongshan Co., Beijing, China). Finally, the sections were visualized with 3-3'-diaminobenzidine, counterstained with haematoxylin and mounted. The samples were rinsed with PBS between each step.

Evaluation of IHC staining

IHC tissue staining was evaluated as previously described [13] by 2 pathologists, who assessed the number of positive cells and the intensity of staining. The positive results were judged by semi-quantitative points. The staining intensity scores were 0 (negative), 1 (weak), 2 (medium) and 3 (strong). The percentage of positive cells was scored as 0 (0%), 1 (1-25%), 2 (26-50%) and 3 (>50%). The staining intensity score and the proportional score were added to obtain the total score. A total score ≥3 was considered to represent high expression. A total score <3 was considered to represent low expression.

Statistical analyses

All statistical analyses were conducted using SPSS 19.0 statistical software. A paired t-test was used to compare the serum vitamin D concentrations of OSCC patients before and after cisplatin chemotherapy. Chi-square analyses were used to examine the correlation between GSDME expression in tumour and ANC tissues. Fisher's exact test was used to examine the relationships between GSDME expression and xenograft mouse sample features. Student's t-test was used to compare the PCR results, cell apoptosis, tumour xenograft results, and cell functions (proliferation, migration, invasion, etc.) between two different groups, ANOVA test was used when more than two sample groups are compared. Unless otherwise noted, quantitative data are expressed as the mean and standard deviation (S.D.). Statistical significance was determined with: *P<0.05; **P<0.01; ***P<0.001, compared with the control.

Results

GSDME shows higher expression in ANC tissues of OSCC than in cancerous tissues

Chemotherapeutic side effects often occur in tumour patients. In OSCC nude mice xenograft chemotherapy models, cisplatin successfully inhibited tumour proliferation [13], but the adverse reactions were obvious. The condition of the nude mice gradually deteriorated (**Figures 1A** and S1A) though xenograft shrinkage. The weight of the mice in the cisplatin-treated group was significantly lower than that in the control group. The elevated mouse serum IL-1β and TNF-α levels suggested that pyroptosis might participate in these side effects (**Figure 1B** and **1C**). Hence, pyroptosis-related proteins, gasdermin family protein D (GSDMD) and GSDME), were analysed by IHC in the mouse OSCC xenografts. GSDMD expression and elevation were not significant in either tumour or normal tissues (Figure S1B) during this process. However, GSDME was weakly expressed in tumour tissues but normally expressed in most normal tissues (**Figures 1D-I**, S1C; **Table 1**). When cisplatin was applied, GSDME expression was elevated in the tongue, skin, stomach, and renal tissues, among others; however, some of these findings were not

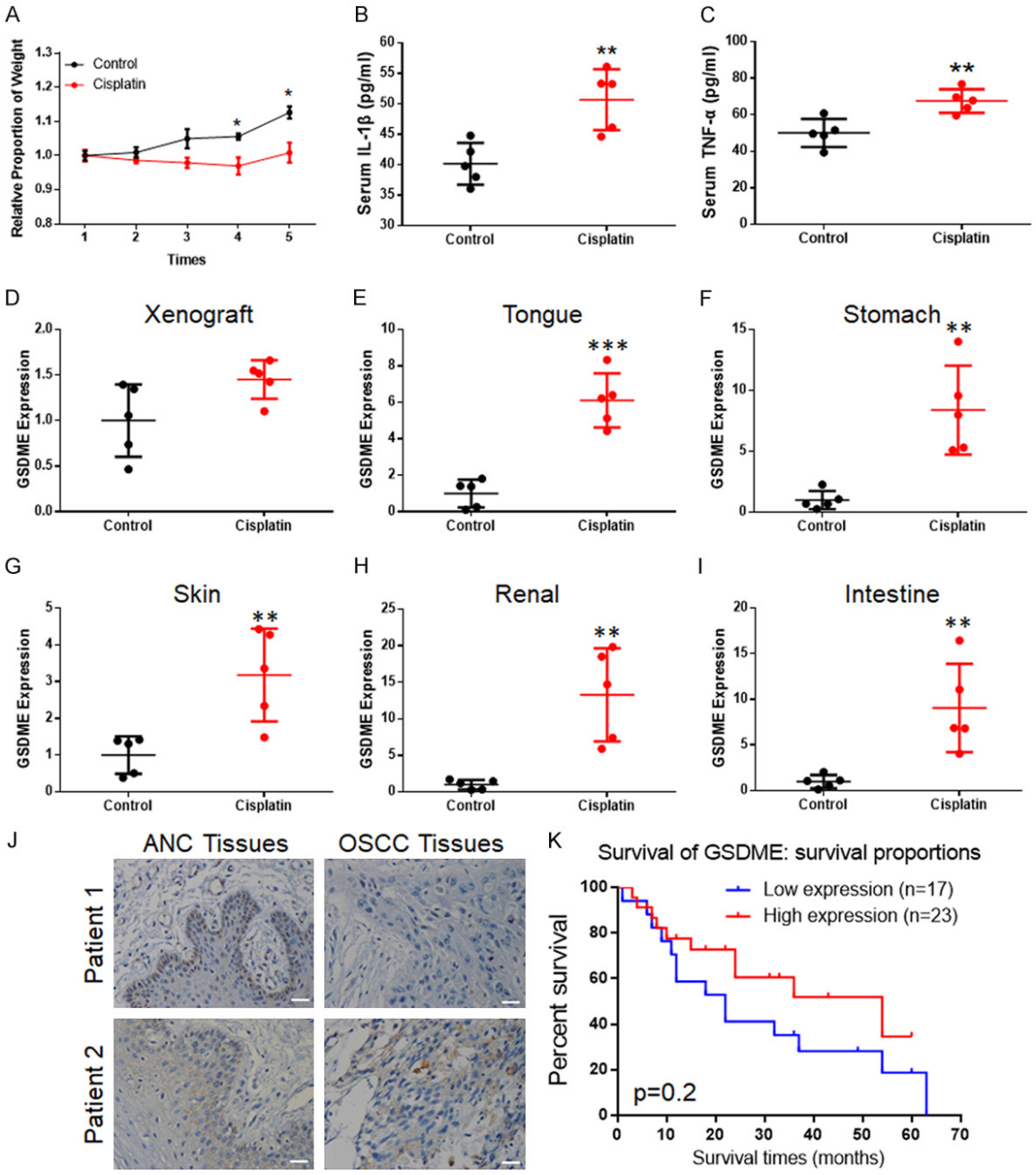

Figure 1. GSDME participated in the regulation of normal tissue cell pyroptosis during cisplatin chemotherapy. (A) After chemotherapy, the weights of OSCC xenograft mice decreased significantly; (B) Elevated serum IL-1β concentrations were detected in cisplatin-treated mice; (C) Elevated serum TNF-α concentrations were detected in cisplatin-treated mice; (D-I) PCR detection of GSDME expression in xenograft (D), tongue (E), stomach (F), skin (G), kidneys (H) and intestine (I), showing GSDME-mRNA significant increased except for in the xenograft; (J) Typical OSCC patient sample IHC of GSDME: patient 1: positive GSDME expression in ANC tissues and negative expression in OSCC tissues; patient 2: positive GSDME expression in both ANC and OSCC tissues (200 ×, scale bar size: 20 μm). (K) Kaplan-Meier estimates of the overall survival of OSCC patients with GSDME expression; the results showed the trend of high expression of OSCC with poorer survival rates, but significant *P* values were not obtained.

statistically significant. Although this increasing trend was not significant in OSCC tissues, elevated GSDME expression in perivascular tissues was observed (Figure S1C, arrow).

To verify the expression of GSDME in OSCC, 40 OSCC tissues and their corresponding ANC tissues were collected for immunohistochemical staining. The different GSDME expression lev-

Table 1. Association of GSDME expression in the samples of xenograft mice during cisplatin-based therapy

Group	GSDME expression			*P* Value
	Low	Moderated	High	
Xenograft				
Control	3	2	0	
Cisplatin	1	3	1	0.333
Tongue				
Control	1	3	1	
Cisplatin	0	1	4	0.140
Skin				
Control	1	2	2	
Cisplatin	0	1	4	0.368
Stomach				
Control	2	3	0	
Cisplatin	0	1	4	0.030
Renal				
Control	1	2	2	
Cisplatin	0	1	4	0.368
Intestine				
Control	0	2	3	
Cisplatin	0	1	4	0.526

els between cancerous and adjacent tissues were statistically significant at 57.5% (23/40) in OSCC tissues and 85% (34/40) in ANC tissues (**Table 2**; **Figure 1J**). The expression of GSDME in OSCC was not significantly related to gender, age, or tumour differentiation in OSCC patients (**Table 3**). Although lymph node metastasis was not statistically significant at 0.066, this finding might have been caused by insufficient samples. However, compared with the prognosis of patients, there was no significant change in the survival time of GSDME and patients (**Figure 1K**), which was similar to the database results (http://gepia.cancer-pku.cn/).

Therefore, the above results suggested that the side effects might originate from GSDME-related destruction of normal tissues by cisplatin.

GSDME-mediated pyroptosis occurs in normal tissue cell lines during cisplatin-based chemotherapy

Regarding oral cancer, oral mucosal reaction and gastrointestinal discomfort are the most common complications during chemotherapy after OSCC surgery. Therefore, we used NOKs and GSEs. We simultaneously observed abnormal expression of GSDME in peritumoural vascular tissues; thus, we included HUVECs as well.

A high-intensity confocal microscope was used for dynamic capture during cell line treatment with cisplatin (**Figure 2A**). During the cell death process, cells exhibited bubble-shaped [14] (a typical form of pyroptosis) death after cisplatin treatment. The elevated secretion of IL-1β in the cisplatin treatment group was detected by enzyme-linked immunosorbent assay (ELISA, **Figure 2B**), as was the elevated concentration of lactate dehydrogenase (LDH, cytotoxicity assessment) in the culture medium (**Figure 2C**).

Then, GSDME was analysed by immunoblot and PCR (**Figure 2D** and **2E**). Cisplatin significantly induced cleavage of GSDME (bands at 35 kDa). Based on both the cleaved and full-length (55 kDa) bands, GSDME expression was upregulated after cisplatin treatment.

The cell line evidence indicated that cisplatin caused the cleavage of GSDME in normal tissue cells and induced normal tissue pyroptosis, which finally produced chemotherapy side effects.

Upregulated GSDME expression results in a decrease in cisplatin tolerance in noncancerous cells

The enhanced expression of GSDME could be caused by a series of stimuli from chemotherapy drugs. To examine cell function alterations when GSDME was highly expressed, GSDME overexpression (GSDME-ov) cell lines using NOKs, GSEs and HUVECs were constructed and verified by immunoblot analysis (**Figure 3A**) and PCR (Figure S2A). The chemotolerance of stable cells was significantly decreased following GSDME upregulation (**Figure 3E**). Subsequently, the GSDME-ov cells were treated with ½ IC50 concentrations of cisplatin. Flow cytometry (Annexin V/PI, **Figures 3G** and **3I**) and cytotoxicity assessments (**Figure 3B**) were performed after 48 hours. Compared with the control group, the cell death rate of GSDME-ov cells increased in the presence of the same

Table 2. GSDME expression in OSCC and ANC tissues

Source	High expression	Low expression	High (%)	*P* value
OSCC	23	17	57.5	
ANC Tissues	34	4	85	0.03

Table 3. Association of GSDME expression with the features of OSCC patients

Characteristics	GSDME expression		*P* Value
	High (%)	Low (%)	
Age			
≤40	12 (70.6)	5 (29.4)	
>40	11 (47.8)	12 (52.2)	0.185
Gender			
Male	11 (50.0)	11 (50.0)	
Female	12 (66.7)	6 (33.3)	0.301
Differentiation			
Well	8 (50.0)	8 (50.0)	
Moderate	9 (60.0)	6 (40.0)	
Poor	6 (66.7)	3 (33.3)	0.414
Lymphatic metastasis			
No	8 (42.1)	11 (57.9)	
Yes	15 (71.4)	6 (28.6)	0.063
Clinical stage (T)			
1	8 (72.7)	3 (27.3)	
2	5 (38.4)	8 (61.5)	
3	7 (70.00)	3 (30.00)	
4	3 (50.00)	3 (50.00)	0.688

GSDME positive 23 (57.5%), negative 17 (42.5%).

cisplatin concentration, and more LDH was excreted.

The sgRNA targeting GSDME was applied to stably inhibit GSDME expression in noncancerous cells. Immunoblot and qPCR analyses were applied to confirm the decreased expression of GSDME in cells (**Figures 3C** and S2B). The cisplatin tolerance of sgGSDME cells was detected as described above. Inhibition of GSDME resulted in an enhancement of chemotolerance (**Figure 3F**) and significantly reduced cell death rates during cisplatin treatment (**Figure 3D**, **3H** and **3J**). HUVECs displayed the same trends (Figures S3).

However, upregulation (Figure S2C) or downregulation (Figure S2D) of GSDME expression did not significantly influence cisplatin tolerance (Figure S2E and S2F) in OSCC cells (CAL-27 and SCC-9). Hence, GSDME mainly played a role in normal tissues.

Inhibiting GSDME cleavage can enhance cisplatin tolerance in normal tissue cells

Protein from the GSDME-ov cell line was collected after cisplatin treatment for immunoblot analysis. Maturation of caspase-3 and cleavage of GSDME were observed after cisplatin treatment (**Figure 4A**), confirming that GSDME-mediated pyroptosis occurred during this process. Whether inhibiting GSDME cleavage can enhance cellular chemo-tolerance remains unknown.

For further clarification, we mutated the cleavage sequence recognized by caspase-3 [15] into the linker sequence of GSDME (**Figure 4B**). GSDME-wild-type (wt) and mutant (-mut) lentiviruses were transfected into GSDME knockout cells (constructed using sgRNA targeted GSDME, Figure S5A and S5C). The extraction of cellular DNA for sequencing confirmed that the GSDME-wt and GSDME-mut sequences were successfully inserted into the cellular genome. Immunoblot analysis showed that during cisplatin treatment, the mutant GSDME protein did not affect the mature caspase-3, but it could not be cleaved during this process (**Figure 4C**). When treating with gradient concentrations of cisplatin, GSDME-mut groups were more tolerant to cisplatin than GSDME-wt ones (**Figures 4D**, **4E** and S4B). FCM results confirmed this trend (**Figure 4H** and **4I**). Furthermore, the GSDME-wt cell lines displayed typical pyroptotic bubbles, while the GSDME-mut cell lines displayed other death shapes, such as shrinkage (**Figures 4F**, **4G**, S4A and S4C).

Therefore, trying to inhibit GSDME cleavage in normal cells during cisplatin chemotherapy could be an effective therapeutic strategy.

Inhibition of caspase-associated inflammatory signals by vitamin D can effectively inhibit pyroptosis from normal tissue

To explore potential strategy for minimizing side effects by pyroptosis, several FDA-approved compounds previously reported to have anti-inflammatory function were tested for inhibition of the source of GSDME-mediated pyroptosis. Classic nonsteroidal anti-inflammatory drugs

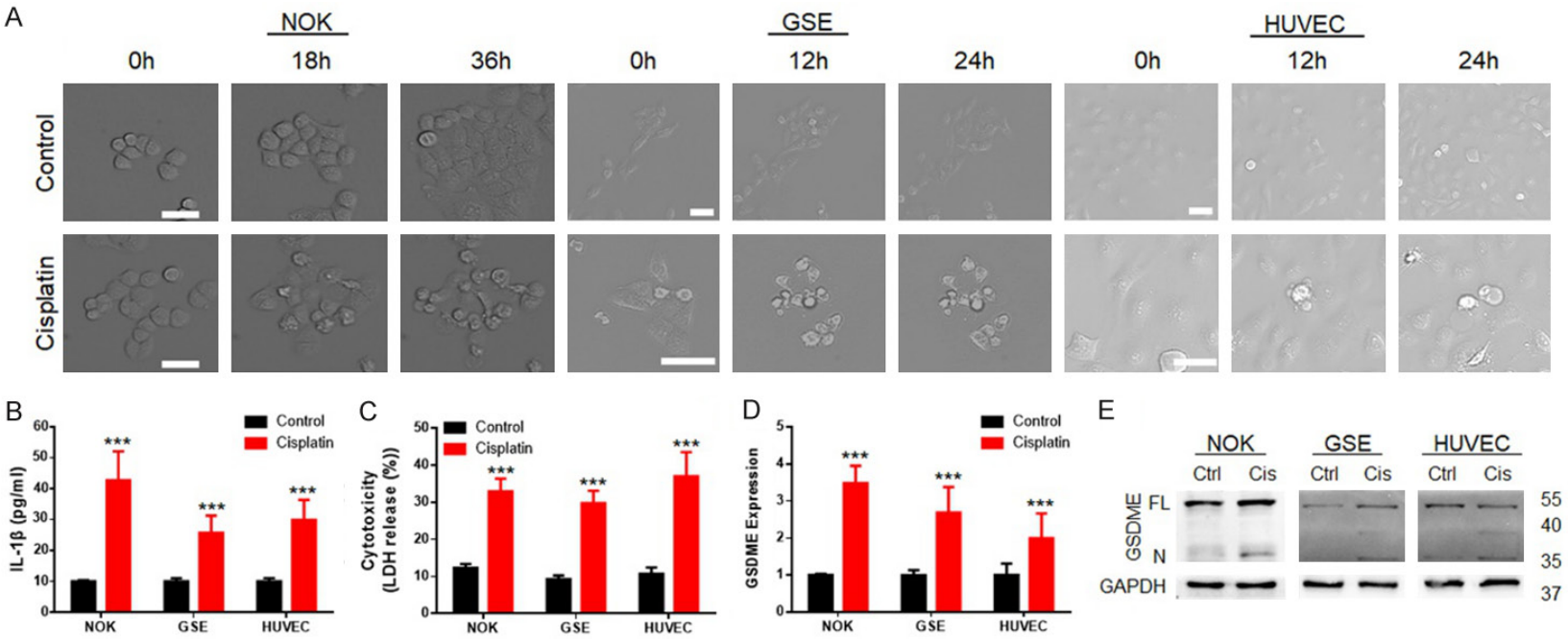

Figure 2. GSDME participated in the regulation of pyroptosis in normal tissue cells during cisplatin-based chemotherapy. A. Microscope capture during the cell death process induced by cisplatin; the tested cells exhibited bubble-shaped death after cisplatin treatment (scale bar size: 50 μm). B. ELISA revealed elevated IL-1β expression in NOKs, GSEs and HUVECs; after cisplatin treatment; C. Cytotoxicity assay showing elevated LDH release in NOKs, GSEs and HUVECs after cisplatin treatment; D. PCR detection revealed that GSDME expression was upregulated in normal tissue cells after cisplatin treatment; E. Immunoblot showed the cleavage of GSDME (35 kDa) during cisplatin treatment of NOKs, GSEs and HUVECs; (cisplatin treatment: NOK 30 μM; GSE 20 μM; HUVEC 40 μM, 24 hours).

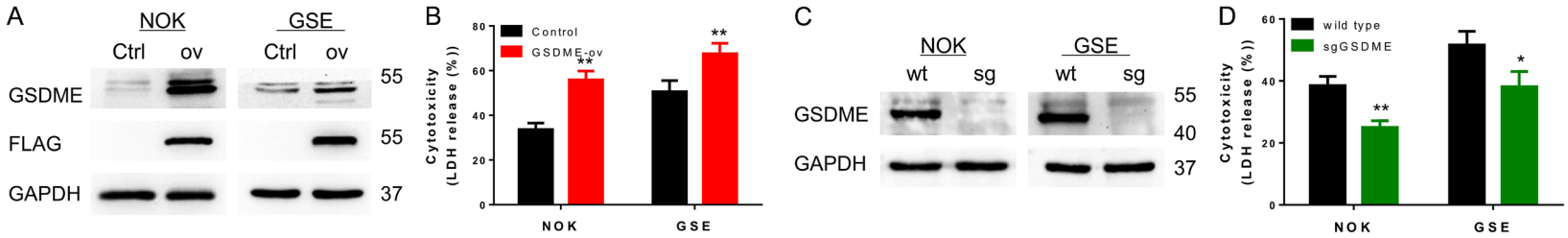

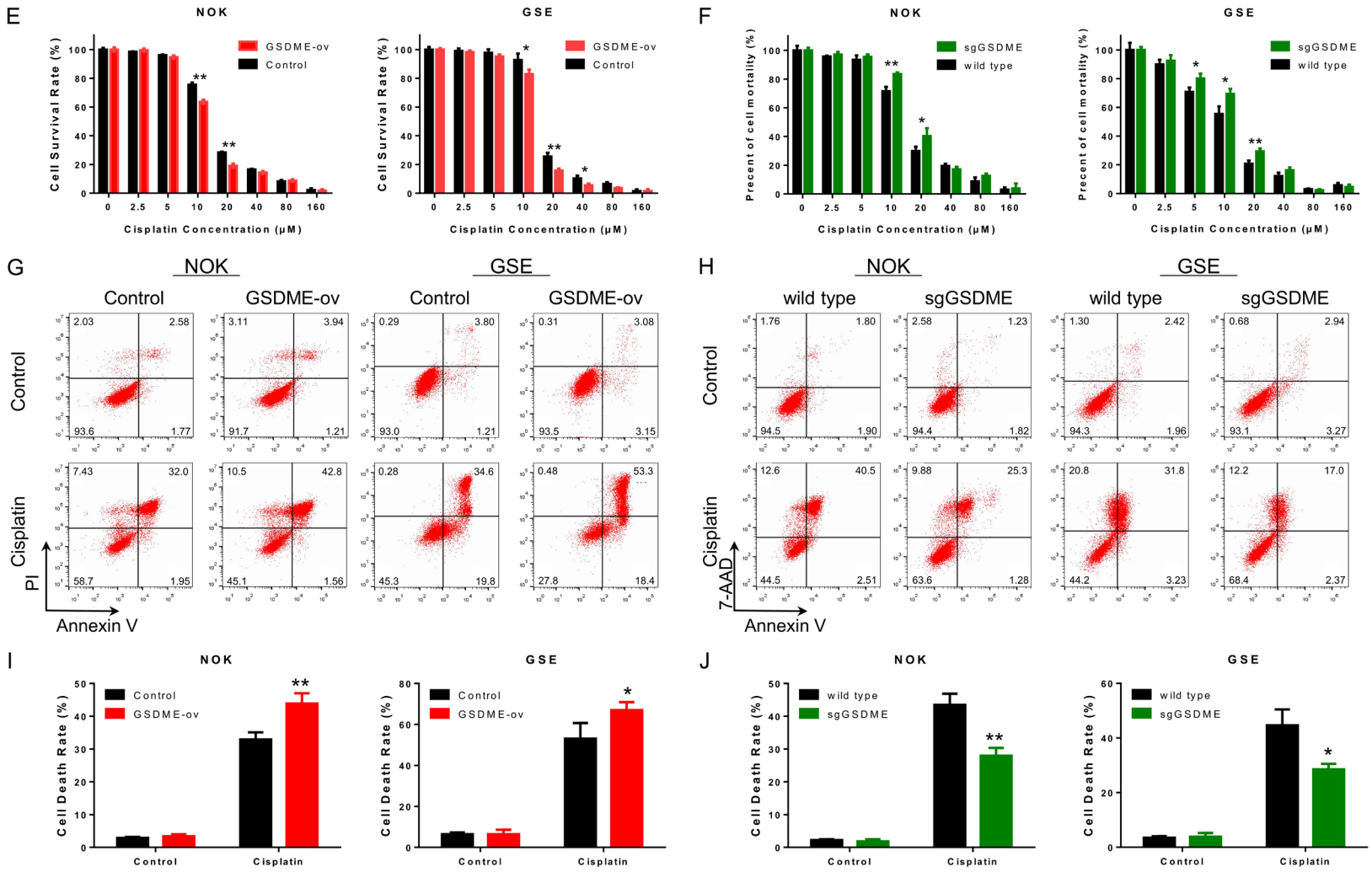

Figure 3. Cellular cisplatin tolerance was increased with downregulation of GSDME expression and vice versa. A. Immunoblot confirmed that GSDME was overexpressed in NOKs and GSEs; the Flag-tag was successfully fused to GSDME; B. The cytotoxicity assay revealed elevated LDH release in GSDME-overexpressing cells compared with control cells after cisplatin treatment, suggesting more GSDME-ov cell death at the same cisplatin concentration; C. Immunoblot analysis confirmed that GSDME was knocked out by GSDME sgRNA in NOKs and GSEs; D. The cytotoxicity assay revealed decreases in LDH release in GSDME knockout cells compared with control cells after cisplatin treatment; E. Gradient concentration of cisplatin-treated GSDME-overexpressing cell lines; cisplatin tolerance was decreased in NOKs and GSEs; F. Gradient concentration of cisplatin-treated NOKs and GSEs with GSDME knockout group; increased cisplatin tolerance was detected; G. FCM detected the cisplatin-sensitive effect on GSDME-overexpressing cell lines using NOKs and GSEs; H. FCM detected the cisplatin-tolerant effect on the GSDME knockout cell line using NOKs and GSEs; I. Statistical analysis of cell death rates of G; cisplatin induced more cell death in GSDME-overexpressing cell lines; J. Statistical

analysis of cell death rates of H; GSDME knockout cell lines were more tolerant during cisplatin treatment. (cisplatin treatment: NOK 30 μM; GSE 20 μM; HUVEC 40 μM, 24 hours for B, D, G, H).

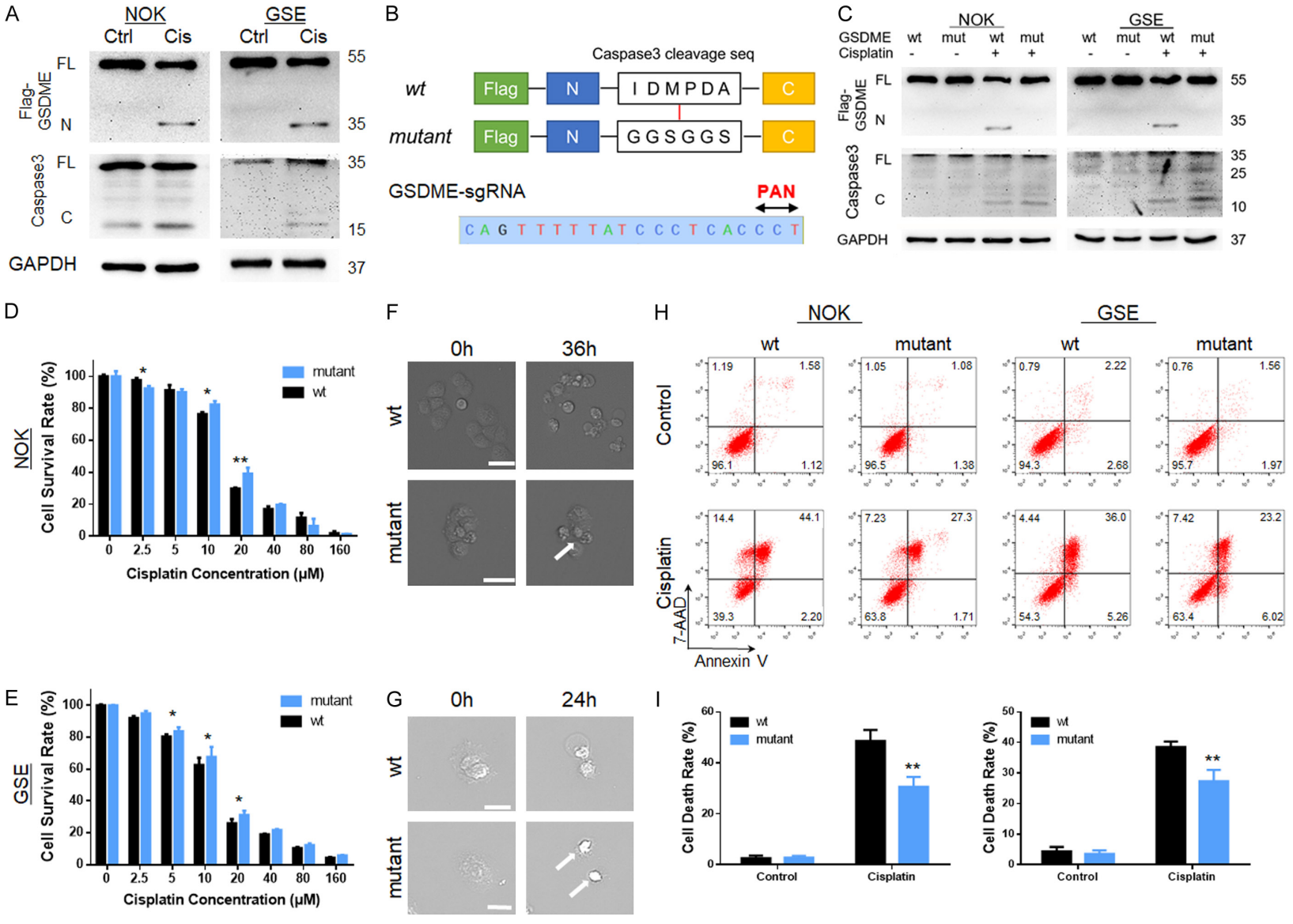

Figure 4. GSDME cleavage was a key factor for cisplatin tolerance alteration in normal tissue cells during cisplatin treatment. A. Immunoblot analysis of GSDME cleavage (35 kDa) and cleaved caspase-3 (15 kDa) expression during cisplatin treatment of NOKs and GSEs with GSDME overexpression; B. GSDME mutant design: the caspase-3 cleavage sequence "IDMPDA" was mutated into the "GGSGGS" linker sequence; GSDME sgRNA and its PAN sequence; C. Immunoblot analysis of GSDME protein cleavage during cisplatin treatment. The GSDME mutant was not cleaved during this process, while the maturation of caspase-3 was not affected; D, E. Gradient concentration of the cisplatin-treated GSDME-wt and GSDME-mut cell lines of NOKs and GSEs; the GSDME-mut cell line was more tolerant than the GSDME-wt cell line; F, G. Microscope capture during the cell death process induced by cisplatin; GSDME-wt cells exhibited pyroptotic death after cisplatin treatment while the mutant group displayed shrinkage shapes (scale bar size: 50 μm); H, I. FCM detected the cisplatin-tolerant effect on the GSDME-wt/mut cell line; under same concentration, cisplatin induced more cell death in GSDME-wt group; (cisplatin treatment: NOK 30 μM; GSE 20 μM, 24 hours for A, C, F, G, and H).

(NSAIDs, aspirin and celecoxib), a glucocorticoid (hydrocortisone) and vitamins (vitamins C and D) were selected. After pre-treatment with the indicated drugs for 3 days, GSDME-ov cells (NOKs, HUVECs and GSEs) were treated with the indicated cisplatin dose for 48 hours. Cell mortality was analysed by flow cytometry (annexin V/PI, **Figures 5A**, **5B**, S6A and S6B). Intriguingly, celecoxib induced a significant increase in cell death, while aspirin, hydrocortisone and vitamin C weakly affected cellular cisplatin tolerance. Among these factors, vitamin D displayed enhanced cisplatin chemotherapy tolerance in both cell lines.

In this research, we selected vitamin D for further studies. The secretion of IL-1β in NOKs, GSEs and HUVECs was significantly increased after cisplatin treatment but remained stable with vitamin D pre-treatment. When cisplatin and vitamin D were combined, cellular IL-1β expression was decreased in the treated group compared with the cisplatin group but was similar to that in the control group (**Figures 5C**, S6C). Subsequently, cisplatin tolerance was examined in normal cell lines and GSEs after pre-treatment with vitamin D and displayed an enhancement of tolerance (**Figures 5D**, S6D). The cytotoxicity test showed that the release of LDH with vitamin D pre-treatment was less than in the control group at the same cisplatin concentration, suggesting reduced cell death (**Figures 5F**, S6E). Moreover, immunoblot verified the reduction of GSDME cleavage and caspase-3 maturation after vitamin D application (**Figure 5E**).

These results indicate that vitamin D could effectively inhibit GSDME-mediated pyroptosis during chemotherapy by inhibiting caspase-3 signals, which was beneficial for improving the tolerance of normal tissues cells to cisplatin.

A high serum vitamin D concentration may facilitate normal tissue protection and reduces chemotherapeutic side effects

Vitamin D was supplemented as a protective agent in the OSCC xenograft model during chemotherapy. After 5 cycles of drug injection, serum vitamin D concentrations decreased significantly after cisplatin treatment, while vitamin D co-supplementation returned the levels to normal. Regarding weight, the application of vitamin D alleviated the weight loss caused by cisplatin chemotherapy. Adverse reactions, such as a bowed back, thin physique and skin folds, were significantly reduced (**Figure 6A** and **6B**). Although the secretion of IL-1β and TNF-α was still elevated in the vitamin D supplementation group after cisplatin application (**Figure 6C** and **6D**), the difference was not significant compared with the non-cisplatin-treated group and the double blank group. Mouse serum IL-1β and TNF-α concentrations were significantly decreased with the application of vitamin D during cisplatin treatment. In addition, after using vitamin D, the expression of GSDME in normal tissues of chemotherapeutic mice did not show a significant increase when comparing to the control and vitamin D groups (**Figure 6I-O**; **Table 4**). The GSDME expression levels between the vitamin D and vitamin D-cisplatin group remained the same.

Patients with OSCC normally undergo adjuvant cisplatin chemotherapy. We compared serum vitamin D levels in oral cancer patients before and after chemotherapy. The results showed that serum vitamin D levels were significantly decreased after chemotherapy (**Figure 6F** and **6G**). The patients' inflammatory index (white blood cell count, WBC) and serum vitamin D concentration showed a negative correlation (**Figure 6H**).

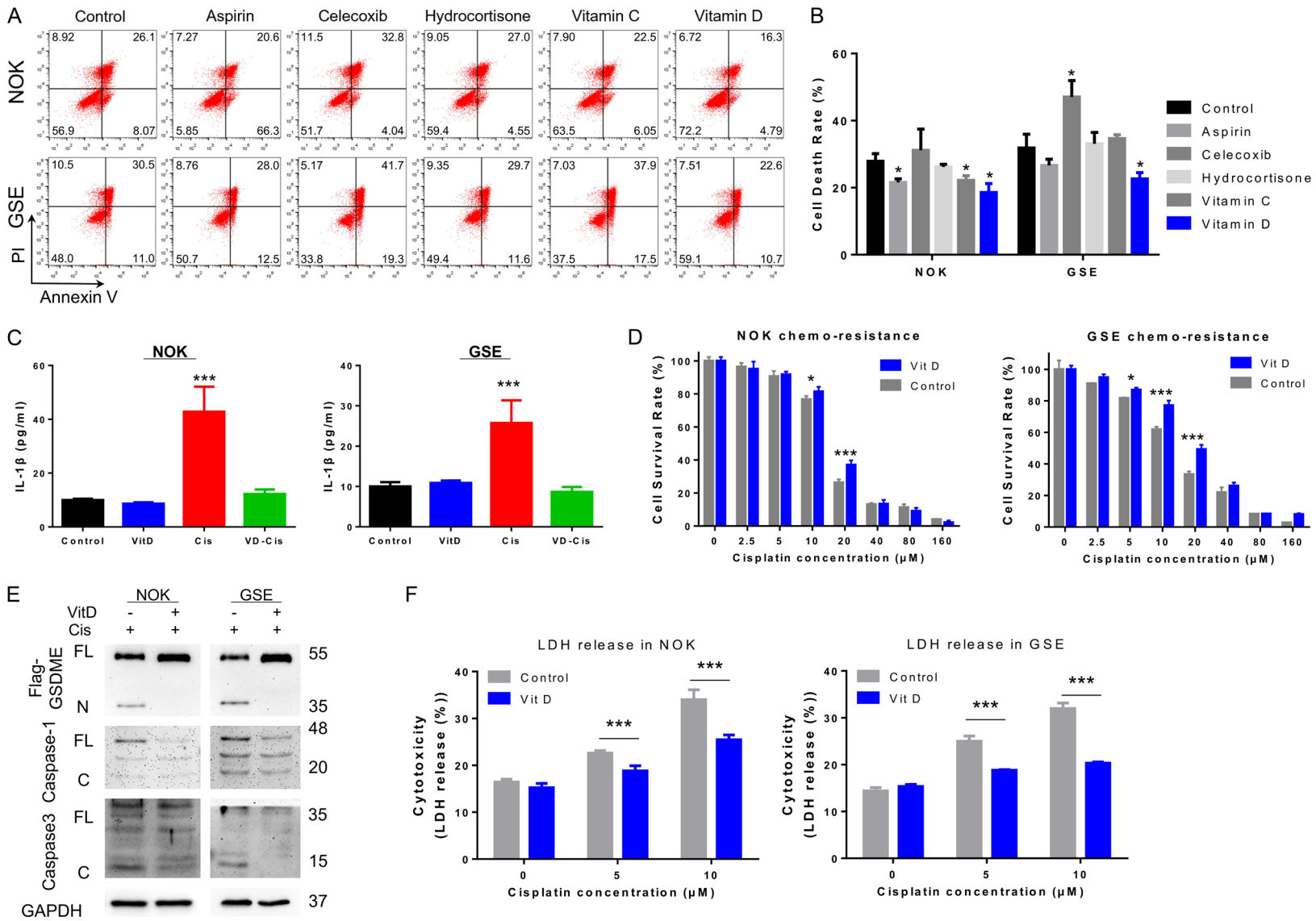

Figure 5. Inhibition of caspase-associated inflammatory signals by vitamin D could effectively inhibit the occurrence of normal tissue cellular pyroptosis. (A) FCM revealed cisplatin-induced cell death in NOKs and GSEs after pre-treatment with aspirin, celecoxib, hydrocortisone, vitamin C and vitamin D; (B) Statistical analysis of the cell death rates shown in (A). Aspirin and vitamin D show the effect of inhibiting cell death during cisplatin treatment; (C) ELISA revealed reduced IL-1β secretion with cisplatin in NOKs and GSEs pre-treated vitamin D; (D) Gradient concentration of cisplatin-treated NOK and GSE pre-treated with vitamin D, which increased cisplatin tolerance; (E) Immunoblot analysis showing that vitamin D pre-treatment could inhibit the cleavage of caspase-1, caspase-3 and GSDME after cisplatin treatment; (F) Cytotoxicity assay revealed that LDH release reduced in NOKs and GSEs pre-treated with vitamin D compared with control cells after cisplatin treatment. (Vitamin D treatment: 30 nM, 3 day; cisplatin treatment: NOK 30 μM; GSE 20 μM, 24 hours for A, C, E, and F).

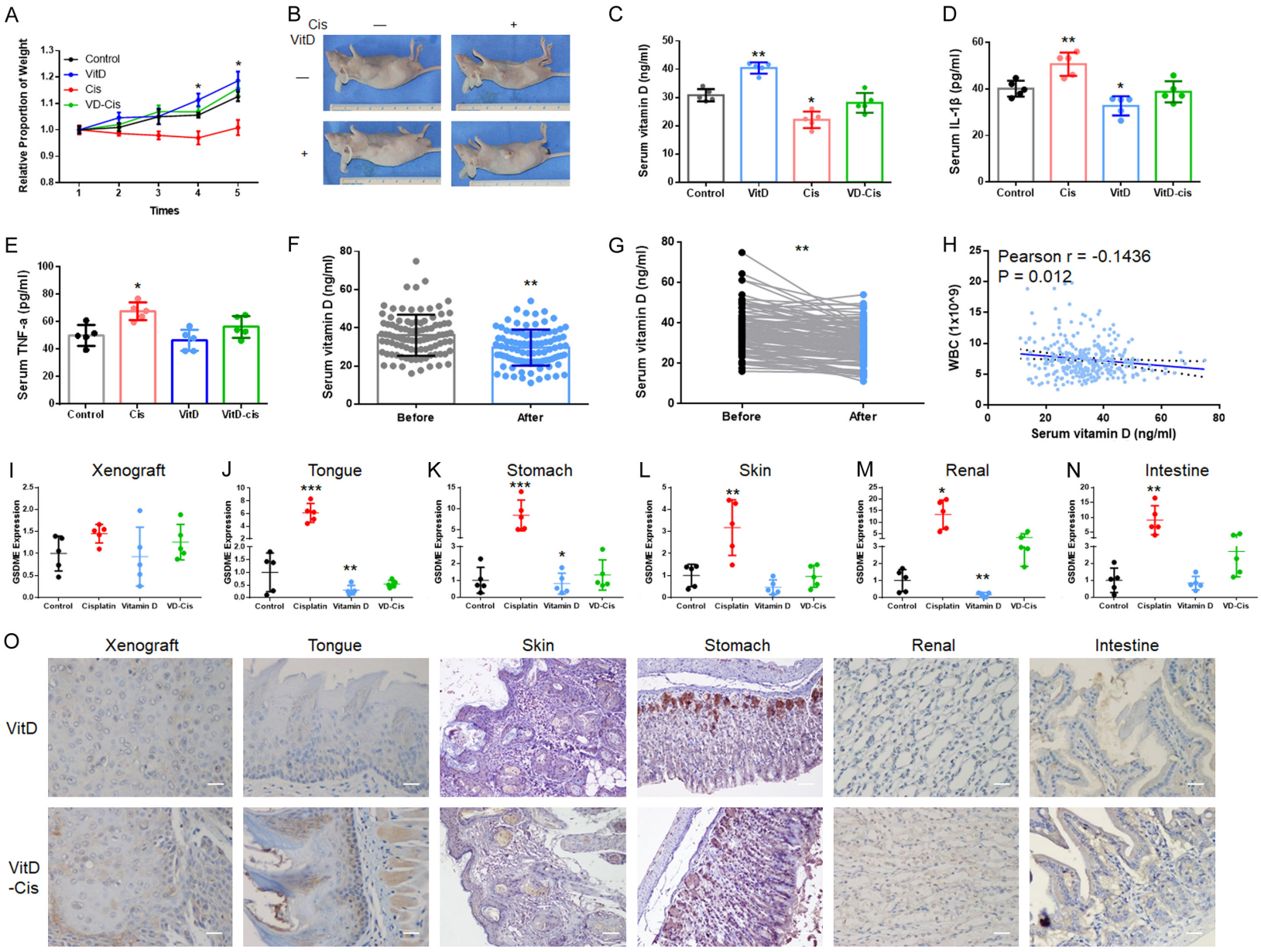
A
Relative Proportion of Weight
Control
VitD
Cis
VD-Cis
Times
B
Cis
VitD
C
Serum vitamin D (ng/ml)
Control
VitD
Cis
VD-Cis
D
Serum IL-1β (pg/ml)
Control
Cis
VitD
VitD-cis
E
Serum TNF-a (pg/ml)
F
Serum vitamin D (ng/ml)
Before
After
G
Serum vitamin D (ng/ml)
H
Pearson r = -0.1436
P = 0.012
WBC (1x10^9)
Serum vitamin D (ng/ml)
I
Xenograft
J
Tongue
K
Stomach
L
Skin
M
Renal
N
Intestine
GSDME Expression
Control
Cisplatin
Vitamin D
VD-Cis
O
Xenograft
Tongue
Skin
Stomach
Renal
Intestine
VitD
VitD -Cis

Figure 6. Serum vitamin D concentration was negatively correlated with the expression of GSDME in OSCC patients and mice. (A) Serum vitamin D concentrations in xenograft mice were detected, and cisplatin treatment reduced serum vitamin D concentrations, while application of vitamin D reversed this effect; (B) With vitamin D supplementation, the weights of OSCC xenograft mice stably increased as the concentration of vitamin D increased during chemotherapy; a hunched back, thin physique and other adverse reactions were not observed; (C) The serum vitamin D concentration of mice were decreased after the treatment of cisplatin. After supplementation with vitamin D, the serum vitamin D remained stable during the cisplatin-vitamin D combined chemotherapy; (D) Elevated serum IL-1β concentrations were detected in vitamin D- and cisplatin-treated mice, but the difference was not significant compared to the control group; (E) Elevated serum TNF-α concentrations were detected in vitamin D- and cisplatin-treated mice, but the difference was not significant compared to the control group; (F, G) In OSCC patients, serum vitamin D levels were significantly decreased after chemotherapy; (H) In OSCC patients, WBC counts showed a negative correlation with serum vitamin D concentrations during chemotherapy; (I-N) PCR detection of GSDME expression in xenograft (I), tongue (J), stomach (K), skin (L), Renal (M) and intestine (N) during the cisplatin-vitamin D combined chemotherapy; (O) Immunohistochemical analysis of GSDME expression in OSCC xenograft mice treated with vitamin D and cisplatin samples, with tumour, tongue, skin, stomach and renal tissues (200 ×, scale bar size: 20 μm).

Table 4. Association of GSDME expression in the samples of xenograft mice pre-treated with vitamin D during cisplatin-based therapy

Group	GSDME expression			*P* Value
	Low	Moderated	High	
Xenograft				
Vitamin D	4	1	0	
VitD-Cis	2	2	1	0.468
Tongue				
Vitamin D	3	2	0	
VitD-Cis	1	3	1	0.333
Skin				
Vitamin D	1	3	1	
VitD-Cis	0	3	2	0.513
Stomach				
Vitamin D	4	1	0	
VitD-Cis	1	3	1	0.150
Renal				
Vitamin D	3	2	0	
VitD-Cis	2	2	1	0.549
Intestine				
Vitamin D	2	3	0	
VitD-Cis	1	3	1	0.513

VitD-Cis: vitamin D-cisplatin.

Discussion

Postoperative chemotherapy is an indispensable and effective method that can be used to improve the prognosis of oral cancer patients [16]. However, the current study found that platinum-based chemotherapy caused normal tissue damage or toxic effects while killing cancer cells, which subsequently induced the associated side effects [17, 18]. Gastrointestinal toxicity, mucosal inflammation, ototoxicity, skin damage, peripheral neuritis, cardiotoxicity, liver damage, and pulmonary fibrosis caused by platinum-based drugs have been widely reported [6, 19, 20]. In particular, for oral cancer patients, the incidence of oral mucositis caused by cisplatin chemotherapy is nearly 100% [9], giving rise to other problems such as local ulcers, periodontitis and gingivitis [21]. In severe cases, it may cause neuropathic pain [22]. Moreover, due to discomfort, it produces the associated health risks and can lead to cancer treatment restraints, such as a dose reduction, cycle delays or even abandonment [23]. The destruction of salivary glands leads to a decrease in salivary secretion and aggravates oral periodontal-gingival diseases [24]. Destruction of the mucosal barrier could lead to the conversion of normal oral-gastrointestinal microflora into viral bacteria, causing a systemic infection [25]. In this study, it was also found that mice treated with cisplatin had a weakened status, with weight loss, debility, and skin shavings.

The elevated secretion of IL-1β and TNF-α from chemotherapy drug-induced mucositis suggests that the side effects of chemotherapy lead to inflammation. Elevated IL-1β and TNF-α levels in the xenograft mouse serum were detected in this research, which confirmed the inflammatory status. High IL-1β secretion indicated that inflammation-related programmed cell death [26], pyroptosis, was involved in these chemotherapeutic side effects.

Pyroptosis was discovered by Senerovic in a study of macrophage cell death induced by

Shigella flexneri [11]. It is a form of programmed cell death that depends on gasdermin proteins [27], which can be cleaved into N- and C-termini. The N-terminus is the functional domain that can bind to cell membrane lipids, causing cell membrane perforation, swelling and death [28]. Then, dead cells release large amounts of inflammatory factors, such as IL-1β and IL-18 [29]. The N-terminus of gasdermin is normally bound to the C-terminus and displays an autoinhibitory effect [30]. Nevertheless, some caspases with cleavage functions that can specifically recognize amino acid sequences linked to the N- and C-termini of gasdermin could lead to its cleavage and the occurrence of pyroptosis. In this study, significant GSDME expression in normal tissues from OSCC patients and xenograft mice suggested that cisplatin-related pyroptosis in normal tissues was mediated by GSDME. Cytological and immunoblot studies have confirmed that cisplatin stimulates GSDME cleavage, increases IL-1β secretion, and displays swelling-shaped cell death in normal tissue cells.

As GSDME expression was higher in normal tissues than in oral cancer tissues, the downregulation of GSDME in noncancerous cells could enhance chemotolerance compared with the control groups, and vice versa. Cisplatin induced caspase-3 production and triggered GSDME-mediated pyroptosis. When caspase-3-cleaved GSDME was inhibited by mutating the cleaved sequence into the linker sequence, cisplatin tolerance was increased. Caspase-3 is produced by the NLP inflammasome through the caspase pathway [31, 32]: inflammasomes induce caspase-1, which in turn stimulates the maturation of caspase-3, resulting in pyroptosis. Moreover, caspase-1 can cleave another gasdermin protein [28], GSDMD, to induce pyroptosis. Since GSDMD was not as widely and strongly expressed as GSDME in normal tissues, inhibiting GSDME cleavage was essential for reducing cisplatin-induced normal tissue pyroptosis, which causes the side effects of platinum-based chemotherapy. Moreover, the presence of inflammation, pyroptosis and normal tissue cell death causes a vicious cycle: IL-1β is released by pyroptosis, which increases the inflammatory environment and triggers pyroptosis, finally aggravating the side effects during tumour chemotherapy.

The difference between GSDME in OSCC and normal cells during cisplatin stimulation is considered related to its upstream NLR family of apoptosis inhibitory protein (NAIP) and its downstream protein called NLRC4. During treatment with cisplatin, NAIP protein upregulates and activates inflammatory signals, resulting in resistance to chemotherapy drugs to inhibit apoptosis. During this process, the increased expression of NLRC4 in turn induces the maturation of caspase-3 and cleavage of GSDME, resulting in pyroptosis. However, according to the results (Figure S5B), the expression of NAIP and NLRC4 was lower in tumour cells than in normal cells. The absence of NAIP-NLRC4 largely reduces caspase-3-GSDME cleavage.

Although direct inhibition of GSDME is an effective way to reduce the side effects of chemotherapy [15, 33, 34], systemic inhibition of GSDME expression is currently difficult to achieve. Hence, the most efficient way to inhibit GSDME-induced cell death and its associated side effects is to suppress the production of caspases [35]; thus, an anti-inflammatory strategy should be implemented [36].

We applied commonly used anti-inflammatory drugs, including aspirin, celecoxib, and hydrocortisone, and anti-tumour vitamins, vitamins C and D, for further research. However, the anti-inflammatory drugs combined with cisplatin had varying effects. Aspirin showed a protective function in HUVECs but not GSE cells, while celecoxib enhanced the cisplatin killing function in both cell types. Although aspirin is an NSAID, it has been reported to inhibit cancer metastasis [37], promoting vascular maturation by inducing endothelial cell autophagy [38]. Additionally, it has damaging effects on the gastric mucosa [39]. The role of celecoxib in tumours remains questionable. It has been reported to inhibit tumour proliferation and metastasis via cyclooxygenase-2 (COX-2) [40] while inhibiting angiogenesis [41]. Nevertheless, some studies have suggested that it can modulate the adhesion of tumour cells and blood vessels, improving the blood-borne dissemination ability of tumours [42]. Moreover, it can improve vascular endothelial cell viability and promote angiogenesis [43]. Hence, aspirin and celecoxib need to be assessed individually to

determine whether they could be used in this situation.

Hydrocortisone is an effective anti-inflammatory drug [44]. However, it has rarely been reported for its role in anti-tumour treatment or angiogenesis. In this study, the effect of normal tissue cells under cisplatin was not significant. Both vitamins C and D have anti-tumour effects [45-47] and anti-inflammatory functions [48]. Vitamin D is more significant than vitamin C. Vitamin D displays enhanced cisplatin chemotherapy tolerance in both cell lines. The cleavage of GSDME, caspase-1 and caspase-3 was significantly reduced after pre-treatment with vitamin D, protecting normal cells from cisplatin destruction. Hence, vitamin D was applied for further studies of normal tissue protection.

The anti-tumour effect of vitamin D has been widely reported in the clinic, and it has also been reported to protect normal tissues [49, 50]. Vitamin D did not affect normal cell growth or development of the animal model while exerting anti-oral tumour effects [51, 52]. It can promote calcium absorption during chemotherapy in breast cancer patients to reduce gastrointestinal reactions [53], similar in that observed in prostate cancer patients [54]. Clinical controlled studies have revealed that vitamin D supplementation can reduce pain and the infectious rate during cancer treatment [55-57]. Moreover, cisplatin treatment promotes bone loss as a side effect, while vitamin D supplementation maintains and restores bone mass in cancer patients [58]. A number of epidemiological studies have found that the higher the plasma vitamin D concentration is in patients with colon cancer, the better their prognosis [59]. However, whether vitamin D inhibits normal tissue pyroptosis in the course of platinum chemotherapy has not yet been reported.

Normal tissue cells were significantly tolerant to cisplatin after pre-treatment with vitamin D in this study. During the course of chemotherapy in mice, vitamin D supplementation resulted in improved conditions. The serum vitamin D concentration decreased after cisplatin chemotherapy but was restored when vitamin D was supplied. The serum IL-1β level in mice displayed the same trend as the serum vitamin D level, suggesting that the inflammatory status of the mice was weakened with high serum vitamin D. In clinical patients, serum vitamin D levels are significantly reduced after chemotherapy. Current research suggests that serum vitamin D concentrations are associated with quality of life in cancer patients [60, 61], reducing cisplatin-based toxicity to normal tissues [62]. Furthermore, high serum vitamin D concentrations have been found to be beneficial for the prevention of osteoporosis [63] and rheumatoid diseases [64], among others. The vitamin D concentration was negatively associated with the WBC count and CRP (i.e., inflammatory indexes for the human body). Therefore, vitamin D supplementation and recovery to its normal serum level should be an important strategy to inhibit the inflammatory response and to reduce the side effects associated with platinum drugs.

In conclusion, this study clarified that the side effects of postoperative chemotherapy in OSCC patients originated from GSDME-mediated pyroptosis. Platinum-based chemotherapy drugs stimulated the cellular inflammatory response, thereby initiating caspase signalling in normal tissues. The upregulated expression and maturation of caspase-3 subsequently cleaved GSDME to induce pyroptosis, releasing IL-1β and TNF-α to cause secondary inflammation. The application of vitamin D could inhibit caspase-3 production and maturation during chemotherapy, decreasing GSDME cleavage and enhancing normal tissue chemotolerance, thereby reducing pyroptosis side effects from cisplatin chemotherapy. A graphic model of this study is shown (**Figure 7**).

Inhibition of systemic GSDME during chemotherapy is currently unachievable. Hence, vitamin D supplementation is essential for normal tissue protection in OSCC patients undergoing chemotherapy. Moreover, the current results suggested that physicians might lessen the dosage of chemotherapy drugs in OSCC patients with the application of vitamin D, improving the efficiency of tumour elimination and protecting normal tissues from side effects under safe conditions. However, additional follow-up experiments are needed to support this hypothesis.

Acknowledgements

This work was supported by grants from National Natural Science Foundation of China

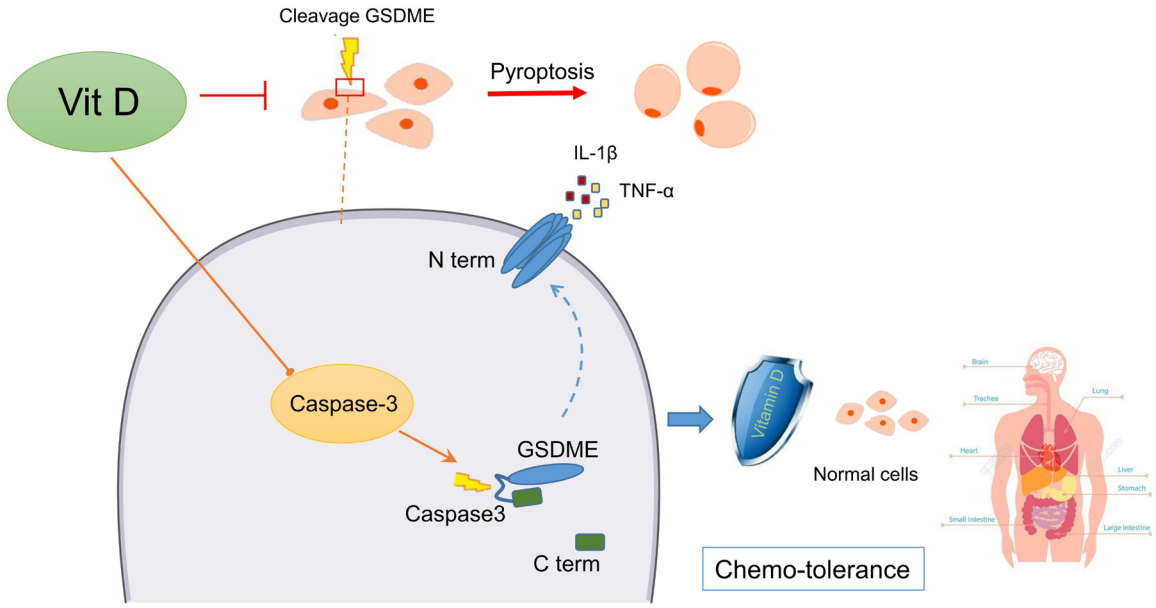

Figure 7. Schematic model of the mechanism by which vitamin D protects normal tissues during cisplatin-based chemotherapy by inhibiting caspase-mediated GSDME cleavage. In normal tissue cells, cisplatin-based chemotherapy induces cellular caspase signals, promoting the production and maturation of caspase-3, which subsequently recognizes and cleaves GSDME into the N-terminus and C-terminus. The N-terminus binds to the cell membrane and forms pores connecting the inside and outside of the cell to trigger pyroptosis. Vitamin D inhibits cellular caspase activation and ultimately inhibits pyroptosis in normal tissues. Therefore, it protects normal tissues from chemotherapy drug destruction and reduces the associated side effects.

(#81772892, #31801075), Science and Technology Program of Guangdong (#2018A030310344, #2019A1515011932), Fundamental Research Funds for the Central Universities (#16ykjc17), The Key Laboratory of Malignant Tumor Gene Regulation and Target Therapy of Guangdong Higher Education Institutes, Sun-Yat-sen University (Grant KLB09001), Key Laboratory of Malignant Tumor Molecular Mechanism and Translational Medicine of Guangzhou Bureau of Science and Information Technology ([2013]163). The datasets used for the current study are available from the corresponding author on reasonable request. All data generated or analysed during this study are included in this published article and its supplementary information files.

Disclosure of conflict of interest

None.

Abbreviations

OSCC, oral squamous cell carcinoma; GSDME, gasdermin family protein E; GSDMD, gasdermin family protein D; NOK, Normal oral squamous epithelial cells; HUVEC, human umbilical vein endothelial cell; GSE, gastric squamous epithelial cells; FCM, flow cytometry; LDH, lactate dehydrogenase; VitD, vitamin D; Cis, cisplatin; ANC, adjacent noncancerous; IHC, Immunohistochemistry; GSDME-ov, GSDME overexpression; shGSDME, shRNA-target GSDME; wt, wild-type; mut, mutant; NSAIDs, nonsteroidal anti-inflammatory drugs; WBC, white blood cell count.

Address correspondence to: Dr. Zhiquan Huang, Department of Oral and Maxillofacial Surgery, Sun Yat-sen Memorial Hospital, 107th Yanjiang Xi Road, Guangzhou 510120, Guangdong, China. E-mail: hzhquan@mail.sysu.edu.cn; zhiquanhuang1978@126.com; Dr. Yin Zhang, Medical Research Center, Sun Yat-sen Memorial Hospital, Sun Yat-sen University, Guangzhou 510120, Guangdong, China. E-mail: zhangy525@mail.sysu.edu.cn

References

[1] Siegel RL, Miller KD and Jemal A. Cancer Statistics, 2017. CA Cancer J Clin 2017; 67: 7-30.
[2] Montero PH and Patel SG. Cancer of the oral cavity. Surg Oncol Clin N Am 2015; 24: 491-508.
[3] Chen W, Zheng R, Baade PD, Zhang S, Zeng H, Bray F, Jemal A, Yu XQ and He J. Cancer statistics in China, 2015. CA Cancer J Clin 2016; 66: 115-132.

[4] Cohen EE, Karrison TG, Kocherginsky M, Mueller J, Egan R, Huang CH, Brockstein BE, Agulnik MB, Mittal BB, Yunus F, Samant S, Raez LE, Mehra R, Kumar P, Ondrey F, Marchand P, Braegas B, Seiwert TY, Villaflor VM, Haraf DJ and Vokes EE. Phase III randomized trial of induction chemotherapy in patients with N2 or N3 locally advanced head and neck cancer. J Clin Oncol 2014; 32: 2735-2743.

[5] Zhong LP, Zhang CP, Ren GX, Guo W, William WJ, Sun J, Zhu HG, Tu WY, Li J, Cai YL, Wang LZ, Fan XD, Wang ZH, Hu YJ, Ji T, Yang WJ, Ye WM, Li J, He Y, Wang YA, Xu LQ, Wang BS, Kies MS, Lee JJ, Myers JN and Zhang ZY. Randomized phase III trial of induction chemotherapy with docetaxel, cisplatin, and fluorouracil followed by surgery versus up-front surgery in locally advanced resectable oral squamous cell carcinoma. J Clin Oncol 2013; 31: 744-751.

[6] Oun R, Moussa YE and Wheate NJ. The side effects of platinum-based chemotherapy drugs: a review for chemists. Dalton Trans 2018; 47: 6645-6653.

[7] Clemens E, Brooks B, de Vries A, van Grotel M, van den Heuvel-Eibrink MM and Carleton B. A comparison of the Muenster, SIOP Boston, Brock, Chang and CTCAEv4.03 ototoxicity grading scales applied to 3,799 audiograms of childhood cancer patients treated with platinum-based chemotherapy. PLoS One 2019; 14: e210646.

[8] Song Y, Liu Y, Lin M, Sheng B and Zhu X. Efficacy of neoadjuvant platinum-based chemotherapy during the second and third trimester of pregnancy in women with cervical cancer: an updated systematic review and meta-analysis. Drug Des Devel Ther 2019; 13: 79-102.

[9] Sonis ST, Elting LS, Keefe D, Peterson DE, Schubert M, Hauer-Jensen M, Bekele BN, Raber-Durlacher J, Donnelly JP and Rubenstein EB. Perspectives on cancer therapy-induced mucosal injury: pathogenesis, measurement, epidemiology, and consequences for patients. Cancer 2004; 100: 1995-2025.

[10] Lian Q, Xu J, Yan S, Huang M, Ding H, Sun X, Bi A, Ding J, Sun B and Geng M. Chemotherapy-induced intestinal inflammatory responses are mediated by exosome secretion of double-strand DNA via AIM2 inflammasome activation. Cell Res 2017; 27: 784-800.

[11] Senerovic L, Tsunoda SP, Goosmann C, Brinkmann V, Zychlinsky A, Meissner F and Kolbe M. Spontaneous formation of IpaB ion channels in host cell membranes reveals how Shigella induces pyroptosis in macrophages. Cell Death Dis 2012; 3: e384.

[12] Xia X, Wang X, Cheng Z, Qin W, Lei L, Jiang J and Hu J. The role of pyroptosis in cancer: pro-cancer or pro-"host"? Cell Death Dis 2019; 10: 650.

[13] Huang Z, Zhang Y, Li H, Zhou Y, Zhang Q, Chen R, Jin T, Hu K, Li S, Wang Y, Chen W and Huang Z. Vitamin D promotes the cisplatin sensitivity of oral squamous cell carcinoma by inhibiting LCN2-modulated NF-kappaB pathway activation through RPS3. Cell Death Dis 2019; 10: 936.

[14] Ding J, Wang K, Liu W, She Y, Sun Q, Shi J, Sun H, Wang DC and Shao F. Pore-forming activity and structural autoinhibition of the gasdermin family. Nature 2016; 535: 111-116.

[15] Wang Y, Gao W, Shi X, Ding J, Liu W, He H, Wang K and Shao F. Chemotherapy drugs induce pyroptosis through caspase-3 cleavage of a gasdermin. Nature 2017; 547: 99-103.

[16] Maghami E, Koyfman SA and Weiss J. Personalizing postoperative treatment of head and neck cancers. Am Soc Clin Oncol Educ Book 2018; 38: 515-522.

[17] Lazarevic T, Rilak A and Bugarcic ZD. Platinum, palladium, gold and ruthenium complexes as anticancer agents: Current clinical uses, cytotoxicity studies and future perspectives. Eur J Med Chem 2017; 142: 8-31.

[18] Dilruba S and Kalayda GV. Platinum-based drugs: past, present and future. Cancer Chemother Pharmacol 2016; 77: 1103-1124.

[19] Oun R and Rowan E. Cisplatin induced arrhythmia; electrolyte imbalance or disturbance of the SA node? Eur J Pharmacol 2017; 811: 125-128.

[20] Waissbluth S, Peleva E and Daniel SJ. Platinum-induced ototoxicity: a review of prevailing ototoxicity criteria. Eur Arch Otorhinolaryngol 2017; 274: 1187-1196.

[21] Gusman D, Ervolino E, Theodoro LH, Garcia VG, Nagata M, Alves B, de Araujo NJ, Matheus HR and de Almeida JM. Antineoplastic agents exacerbate periodontal inflammation and aggravate experimental periodontitis. J Clin Periodontol 2019; 46: 457-469.

[22] Addington J and Freimer M. Chemotherapy-induced peripheral neuropathy: an update on the current understanding. F1000Res 2016; 5: F1000 Faculty Rev-1466.

[23] Campos JC, Cunha JD, Ferreira DC, Reis S and Costa PJ. Challenges in the local delivery of peptides and proteins for oral mucositis management. Eur J Pharm Biopharm 2018; 128: 131-146.

[24] Cetiner D, Cetiner S, Uraz A, Alpaslan GH, Alpaslan C, Toygar MT and Karadeniz C. Oral and dental alterations and growth disruption following chemotherapy in long-term survivors of childhood malignancies. Support Care Cancer 2019; 27: 1891-1899.

[25] Khan SA and Wingard JR. Infection and mucosal injury in cancer treatment. J Natl Cancer Inst Monogr 2001: 31-36.
[26] Fink SL and Cookson BT. Apoptosis, pyroptosis, and necrosis: mechanistic description of dead and dying eukaryotic cells. Infect Immun 2005; 73: 1907-1916.
[27] Yang J, Liu Z, Wang C, Yang R, Rathkey JK, Pinkard OW, Shi W, Chen Y, Dubyak GR, Abbott DW and Xiao TS. Mechanism of gasdermin D recognition by inflammatory caspases and their inhibition by a gasdermin D-derived peptide inhibitor. Proc Natl Acad Sci U S A 2018; 115: 6792-6797.
[28] Shi J, Zhao Y, Wang K, Shi X, Wang Y, Huang H, Zhuang Y, Cai T, Wang F and Shao F. Cleavage of GSDMD by inflammatory caspases determines pyroptotic cell death. Nature 2015; 526: 660-665.
[29] Schneider KS, Gross CJ, Dreier RF, Saller BS, Mishra R, Gorka O, Heilig R, Meunier E, Dick MS, Cikovic T, Sodenkamp J, Medard G, Naumann R, Ruland J, Kuster B, Broz P and Gross O. The inflammasome drives GSDMD-independent secondary pyroptosis and IL-1 release in the absence of caspase-1 protease activity. Cell Rep 2017; 21: 3846-3859.
[30] Liu Z, Wang C, Yang J, Zhou B, Yang R, Ramachandran R, Abbott DW and Xiao TS. Crystal structures of the full-length murine and human gasdermin D reveal mechanisms of autoinhibition, lipid binding, and oligomerization. Immunity 2019; 51: 43-49.
[31] Xi H, Zhang Y, Xu Y, Yang WY, Jiang X, Sha X, Cheng X, Wang J, Qin X, Yu J, Ji Y, Yang X and Wang H. Caspase-1 inflammasome activation mediates homocysteine-induced pyrop-apoptosis in endothelial cells. Circ Res 2016; 118: 1525-1539.
[32] Man SM, Karki R and Kanneganti TD. Molecular mechanisms and functions of pyroptosis, inflammatory caspases and inflammasomes in infectious diseases. Immunol Rev 2017; 277: 61-75.
[33] Mai FY, He P, Ye JZ, Xu LH, Ouyang DY, Li CG, Zeng QZ, Zeng CY, Zhang CC, He XH and Hu B. Caspase-3-mediated GSDME activation contributes to cisplatin- and doxorubicin-induced secondary necrosis in mouse macrophages. Cell Prolif 2019; 52: e12663.
[34] Zheng X, Zhong T, Ma Y, Wan X, Qin A, Yao B, Zou H, Song Y and Yin D. Bnip3 mediates doxorubicin-induced cardiomyocyte pyroptosis via caspase-3/GSDME. Life Sci 2020; 242: 117186.
[35] Xue Z, Xi Q, Liu H, Guo X, Zhang J, Zhang Z, Li Y, Yang G, Zhou D, Yang H, Zhang L, Zhang Q, Gu C, Yang J, Da Y, Yao Z, Duo S and Zhang R. miR-21 promotes NLRP3 inflammasome activation to mediate pyroptosis and endotoxic shock. Cell Death Dis 2019; 10: 461.
[36] Li C, Wang X, Kuang M, Li L, Wang Y, Yang F and Wang G. UFL1 modulates NLRP3 inflammasome activation and protects against pyroptosis in LPS-stimulated bovine mammary epithelial cells. Mol Immunol 2019; 112: 1-9.
[37] Dai X, Yan J, Fu X, Pan Q, Sun D, Xu Y, Wang J, Nie L, Tong L, Shen A, Zheng M, Huang M, Tan M, Liu H, Huang X, Ding J and Geng M. Aspirin inhibits cancer metastasis and angiogenesis via targeting heparanase. Clin Cancer Res 2017; 23: 6267-6278.
[38] Zhao Q, Wang Z, Wang Z, Wu L and Zhang W. Aspirin may inhibit angiogenesis and induce autophagy by inhibiting mTOR signaling pathway in murine hepatocarcinoma and sarcoma models. Oncol Lett 2016; 12: 2804-2810.
[39] Alese MO, Adewole SO, Akinwunmi KF, Omonisi AE and Alese OO. Aspirin-induced gastric lesions alters EGFR and PECAM-1 immunoreactivity in wistar rats: modulatory action of flavonoid fraction of musa paradisiaca. Open Access Maced J Med Sci 2017; 5: 569-577.
[40] Tai Y, Zhang LH, Gao JH, Zhao C, Tong H, Ye C, Huang ZY, Liu R and Tang CW. Suppressing growth and invasion of human hepatocellular carcinoma cells by celecoxib through inhibition of cyclooxygenase-2. Cancer Manag Res 2019; 11: 2831-2848.
[41] Raut CP, Nawrocki S, Lashinger LM, Davis DW, Khanbolooki S, Xiong H, Ellis LM and McConkey DJ. Celecoxib inhibits angiogenesis by inducing endothelial cell apoptosis in human pancreatic tumor xenografts. Cancer Biol Ther 2004; 3: 1217-1224.
[42] Dianzani C, Brucato L, Gallicchio M, Rosa AC, Collino M and Fantozzi R. Celecoxib modulates adhesion of HT29 colon cancer cells to vascular endothelial cells by inhibiting ICAM-1 and VCAM-1 expression. Br J Pharmacol 2008; 153: 1153-1161.
[43] Toomey DP, Manahan E, McKeown C, Rogers A, McMillan H, Geary M, Conlon KC and Murphy JF. Vascular endothelial growth factor and not cyclooxygenase 2 promotes endothelial cell viability in the pancreatic tumor microenvironment. Pancreas 2010; 39: 595-603.
[44] Dandona P, Ghanim H, Sia CL, Green K, Abuaysheh S, Dhindsa S, Chaudhuri A and Makdissi A. A mixed anti-inflammatory and pro-inflammatory response associated with a high dose of corticosteroids. Curr Mol Med 2014; 14: 793-801.
[45] Wei L, Wang C, Chen X, Yang B, Shi K, Benington LR, Lim LY, Shi S and Mo J. Dual-responsive, methotrexate-loaded, ascorbic acid-derived micelles exert anti-tumor and anti-metastatic effects by inhibiting NF-kappaB sig-

naling in an orthotopic mouse model of human choriocarcinoma. Theranostics 2019; 9: 4354-4374.
[46] Ramezankhani B, Taha MF and Javeri A. Vitamin C counteracts miR-302/367-induced reprogramming of human breast cancer cells and restores their invasive and proliferative capacity. J Cell Physiol 2019; 234: 2672-2682.
[47] Chen XY, Chen Y, Qu CJ, Pan ZH, Qin Y, Zhang X, Liu WJ, Li DF and Zheng Q. Vitamin C induces human melanoma A375 cell apoptosis via Bax- and Bcl-2-mediated mitochondrial pathways. Oncol Lett 2019; 18: 3880-3886.
[48] Aimo A, Castiglione V, Borrelli C, Saccaro LF, Franzini M, Masi S, Emdin M and Giannoni A. Oxidative stress and inflammation in the evolution of heart failure: from pathophysiology to therapeutic strategies. Eur J Prev Cardiol 2020; 27: 494-510.
[49] Jimenez-Lara AM. Colorectal cancer: potential therapeutic benefits of Vitamin D. Int J Biochem Cell Biol 2007; 39: 672-677.
[50] Duffy MJ, Murray A, Synnott NC, O'Donovan N and Crown J. Vitamin D analogues: Potential use in cancer treatment. Crit Rev Oncol Hematol 2017; 112: 190-197.
[51] Feldman D, Krishnan AV, Swami S, Giovannucci E and Feldman BJ. The role of vitamin D in reducing cancer risk and progression. Nat Rev Cancer 2014; 14: 342-357.
[52] Grant WB. Vitamin D status: ready for guiding prostate cancer diagnosis and treatment? Clin Cancer Res 2014; 20: 2241-2243.
[53] Kilbreath S, Refshauge KM, Beith J, Ward L, Sawkins K, Paterson R, Clifton-Bligh P, Sambrook PN, Simpson JM and Nery L. Prevention of osteoporosis as a consequence of aromatase inhibitor therapy in postmenopausal women with early breast cancer: rationale and design of a randomized controlled trial. Contemp Clin Trials 2011; 32: 704-709.
[54] Davison BJ, Wiens K and Cushing M. Promoting calcium and vitamin D intake to reduce the risk of osteoporosis in men on androgen deprivation therapy for recurrent prostate cancer. Support Care Cancer 2012; 20: 2287-2294.
[55] Helde-Frankling M, Bergqvist J, Klasson C, Nordstrom M, Hoijer J, Bergman P and Bjorkhem-Bergman L. Vitamin D supplementation to palliative cancer patients: protocol of a double-blind, randomised controlled trial 'Palliative-D'. BMJ Support Palliat Care 2017; 7: 458-463.
[56] Helde-Frankling M and Bjorkhem-Bergman L. Vitamin D in Pain Management. Int J Mol Sci 2017; 18: 2170.
[57] Helde-Frankling M, Hoijer J, Bergqvist J and Bjorkhem-Bergman L. Vitamin D supplementation to palliative cancer patients shows positive effects on pain and infections-Results from a matched case-control study. PLoS One 2017; 12: e184208.
[58] Martin-Herranz A and Salinas-Hernandez P. Vitamin D supplementation review and recommendations for women diagnosed with breast or ovary cancer in the context of bone health and cancer prognosis/risk. Crit Rev Oncol Hematol 2015; 96: 91-99.
[59] Dou R, Ng K, Giovannucci EL, Manson JE, Qian ZR and Ogino S. Vitamin D and colorectal cancer: molecular, epidemiological and clinical evidence. Br J Nutr 2016; 115: 1643-1660.
[60] Lim A, Shayan R and Varigos G. High serum vitamin D level correlates with better prognostic indicators in primary melanoma: A pilot study. Australas J Dermatol 2018; 59: 182-187.
[61] O'Brien KM, Sandler DP, Taylor JA and Weinberg CR. Serum vitamin D and risk of breast cancer within five years. Environ Health Perspect 2017; 125: 77004.
[62] Abdel ML, Helmy MW and El-Abhar HS. Co-targeting of endothelin-A and vitamin D receptors: a novel strategy to ameliorate cisplatin-induced nephrotoxicity. Pharmacol Rep 2019; 71: 917-925.
[63] Candido FG and Bressan J. Vitamin D: link between osteoporosis, obesity, and diabetes? Int J Mol Sci 2014; 15: 6569-6591.
[64] Gulyas K, Horvath A, Vegh E, Pusztai A, Szentpetery A, Petho Z, Vancsa A, Bodnar N, Csomor P, Hamar A, Bodoki L, Bhattoa HP, Juhasz B, Nagy Z, Hodosi K, Karosi T, FitzGerald O, Szucs G, Szekanecz Z, Szamosi S and Szanto S. Effects of 1-year anti-TNF-alpha therapies on bone mineral density and bone biomarkers in rheumatoid arthritis and ankylosing spondylitis. Clin Rheumatol 2020; 39: 167-175.

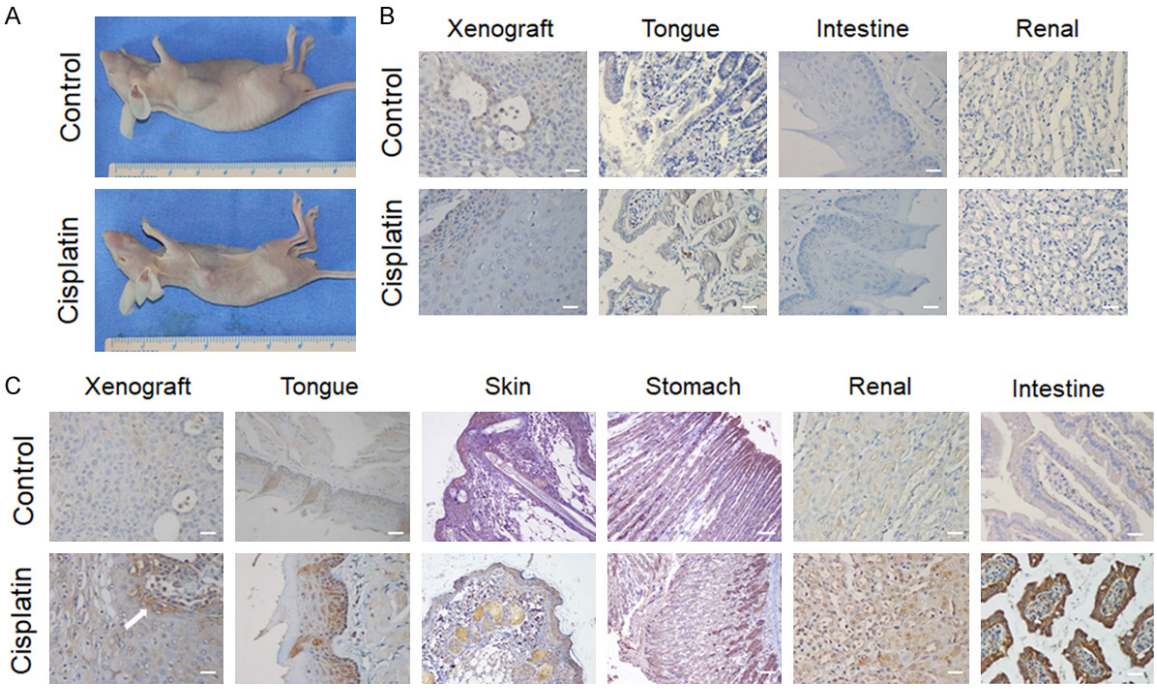

Figure S1. A. After chemotherapy, the mice appeared to have a hunched back, thin physique and other adverse reactions; B. Typical immunohistochemical analysis of GSDMD expression in OSCC xenograft mice samples, with tumour, tongue, intestine and renal tissues. GSDMD did not show an increased trend (scale bar size 20 μm); C. Immunohistochemical analysis of GSDME expression in OSCC xenograft mice samples, with xenograft, tongue, skin, stomach, renal and intestine tissues. After cisplatin treatment, GSDME was high expressed (scale bar size 20 μm).

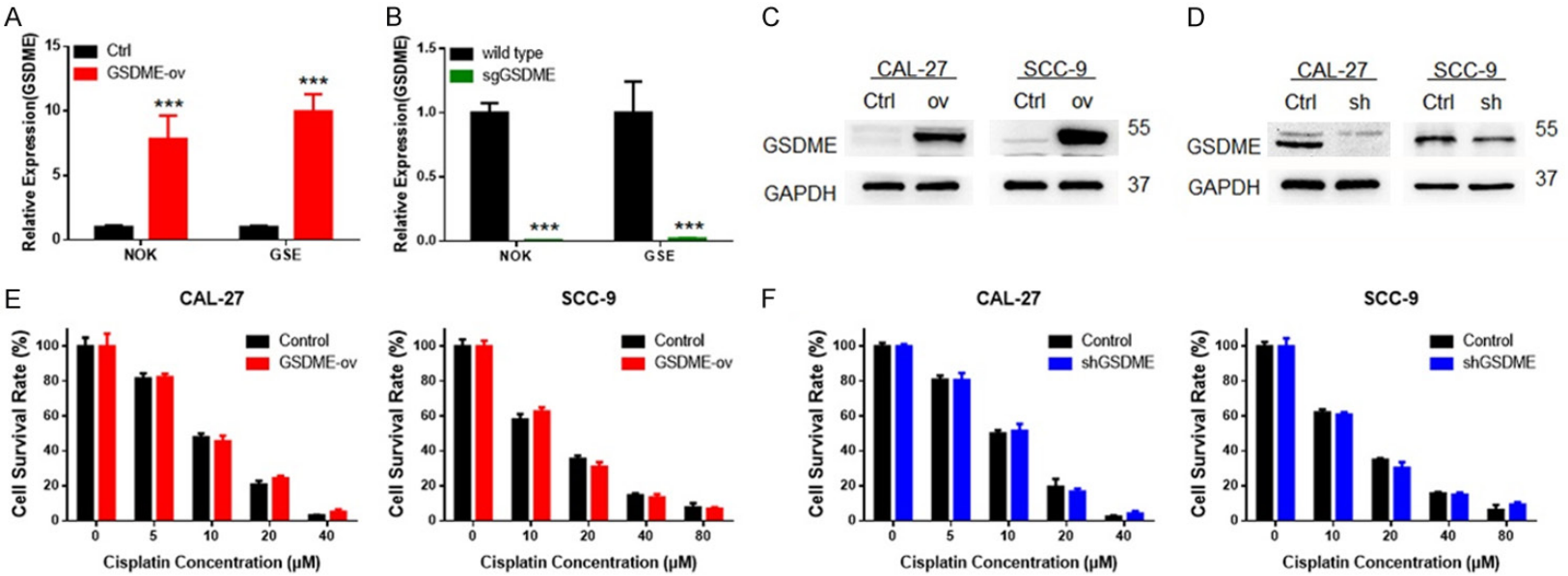

Figure S2. GSDME expression does not affect the sensitivity of OSCC cells to cisplatin chemotherapy. A. PCR confirmed that GSDME was overexpressed in NOKs and GSEs; B. PCR confirmed that GSDME was inhibited in NOKs and GSEs; C. Immunoblot confirmed that GSDME was overexpressed in the OSCC cell line (CAL-27 and SCC-9); D. Immunoblot confirmed that GSDME was inhibited in the OSCC cell line (CAL-27 and SCC-9); E. Gradient concentration of cisplatin-treated GSDME overexpressing OSCC cell lines; increased GSDME expression does not affect the cellular cisplatin sensitivity; F. Gradient concentration of the cisplatin-treated OSCC cell line with inhibited GSDME expression; decreased GSDME expression does not affect the cellular cisplatin tolerance.

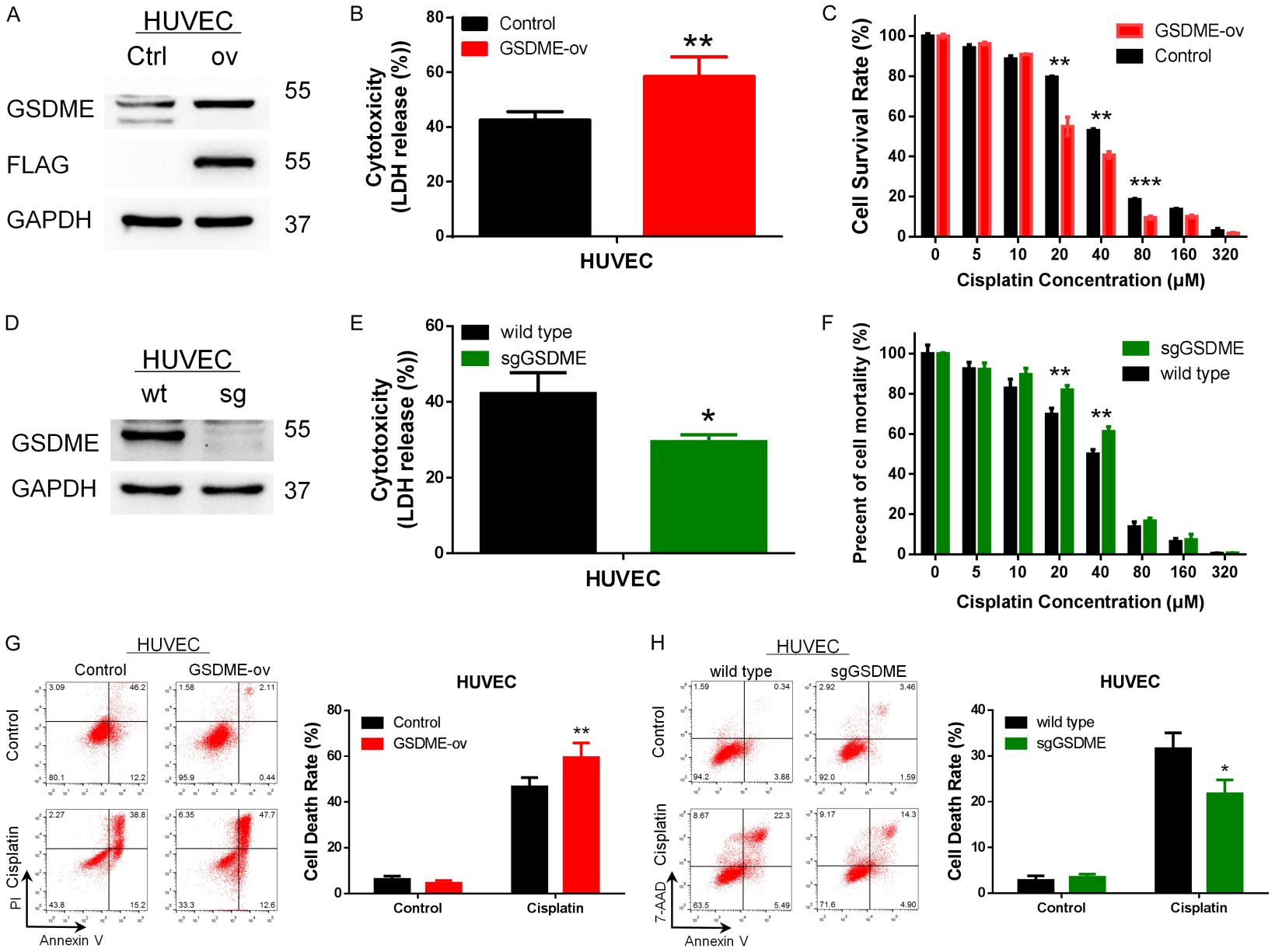
A
HUVEC
Ctrl
ov
GSDME
FLAG
GAPDH
55
55
37
B
Control
GSDME-ov
Cytotoxicity (LDH release (%))
HUVEC
C
GSDME-ov
Control
Cell Survival Rate (%)
Cisplatin Concentration (μM)
D
HUVEC
wt
sg
GSDME
GAPDH
55
37
E
wild type
sgGSDME
Cytotoxicity (LDH release (%))
HUVEC
F
sgGSDME
wild type
Precent of cell mortality (%)
Cisplatin Concentration (μM)
G
HUVEC
Control
GSDME-ov
Control
Cisplatin
PI
Annexin V
Cell Death Rate (%)
H
HUVEC
wild type
sgGSDME
Control
Cisplatin
7-AAD
Annexin V
Cell Death Rate (%)

Figure S3. GSDME expression in HUVECs regulates the chemotherapy sensitivity of these cells. A. Immunoblot confirmed that GSDME was overexpressed in HUVECs; the Flag-tag was successfully fused to GSDME; B. The cytotoxicity assay revealed elevated LDH release in GSDME overexpressing HUVECs compared with control cells after cisplatin treatment; C. Gradient concentration of cisplatin-treated GSDME-ov HUVECs and decreased cisplatin tolerance was confirmed; D. Immunoblot analysis confirmed that GSDME was knockout in HUVECs; E. Cytotoxicity assay revealed decreases in LDH release in GSDME-knockout HUVECs compared with control cells after cisplatin treatment; F. Gradient concentration of cisplatin-treated HUVECs with GSDME knockout, and increased cisplatin tolerance; G. FCM detected the cisplatin-sensitive effect on GSDME-ov cell lines using HUVECs; H. FCM detected the cisplatin-tolerant effect on the GSDME-knockout HUVECs; (cisplatin treatment: 40 μM, 24 hours for B, E, G, and H).

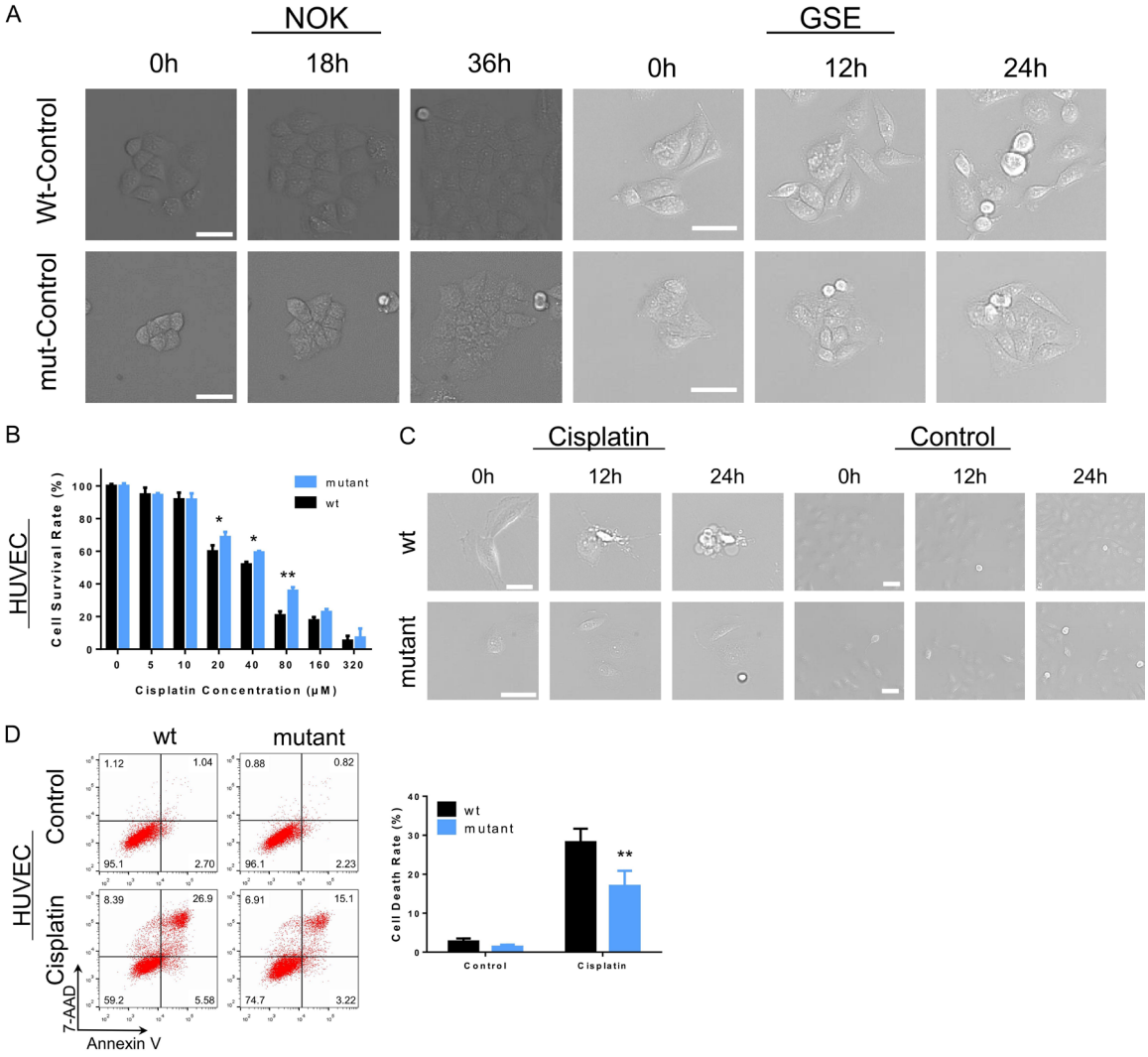

Figure S4. A. Microscope image of GSDME-wt and GSDME-mut cell lines of NOKs and GSEs during cisplatin treatments (control group, scale bar: 50 μm); B. Gradient concentration of cisplatin-treated GSDME-wt/mut HUVECs; the GSDME-mut cell line was more tolerant than the GSDME-wt ones; C. Microscope capture during the cell death process induced by cisplatin of HUVECs GSDME-wt/mutant cell lines (scale bar: 50 μm); D. FCM detected the cisplatin-tolerant effect on the GSDME-wt/mut HUVECs; under same concentration, cisplatin induced more cell death in the GSDME-wt group; (cisplatin treatment: 40 μM, 24 hours for B, C, and D).

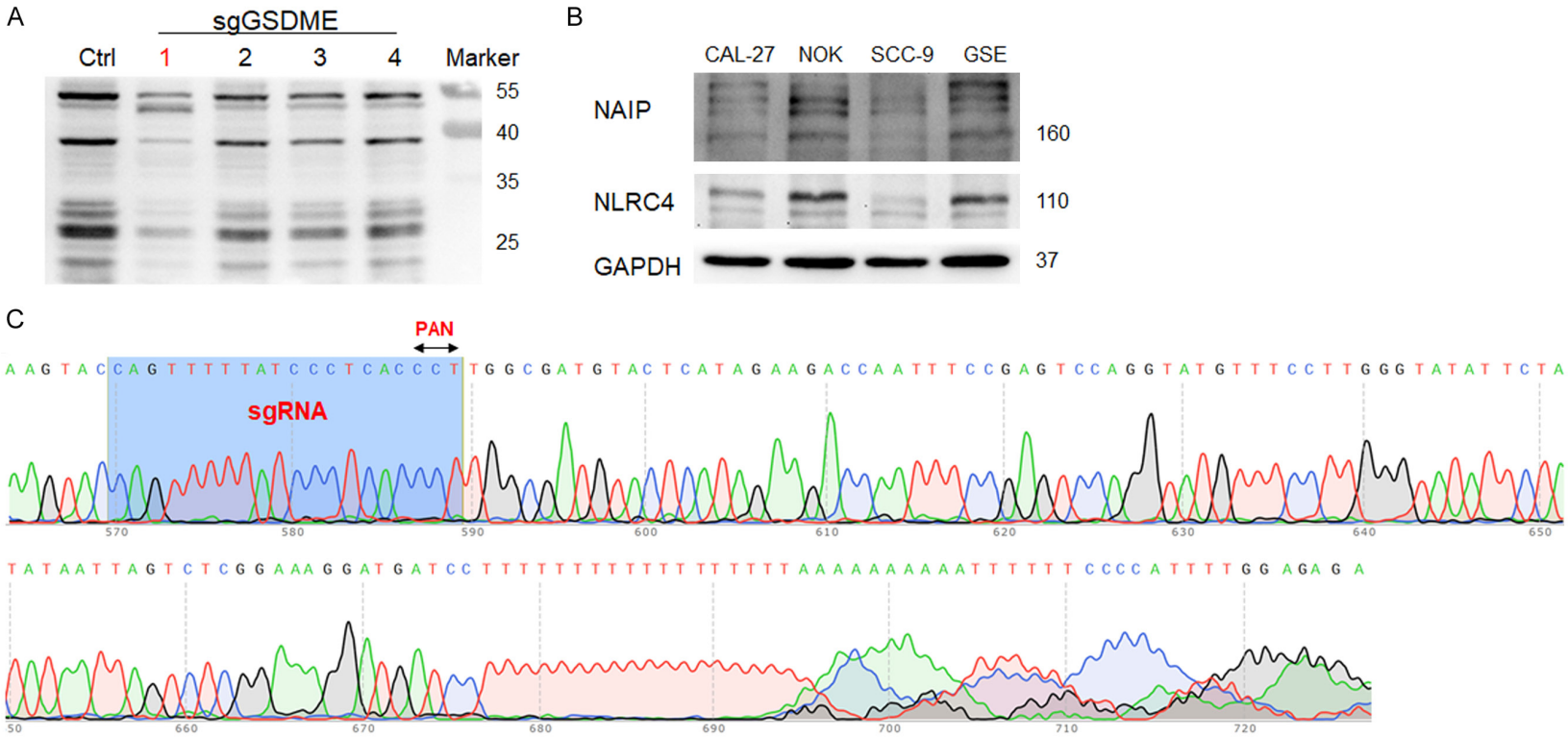

Figure S5. Construction and verification of GSDME knockout cell line. A. After transfecting px458-sgGSDME in NOKs, monoclonal immunoblot was used to detect the expression of GSDME, and clone 1 was selected for sequencing verification; B. Immunoblot detection of NAIP-NLRC4 expression in OSCC tumour cells and normal tissue cells and found that the expression of NAIP-NLRC4 in tumour cells was lower than that in normal tissue cells; C. DNA sequencing of sgGSDME cells; it was found that the sgRNA sequence was truncated, confirming the function of sgRNA.

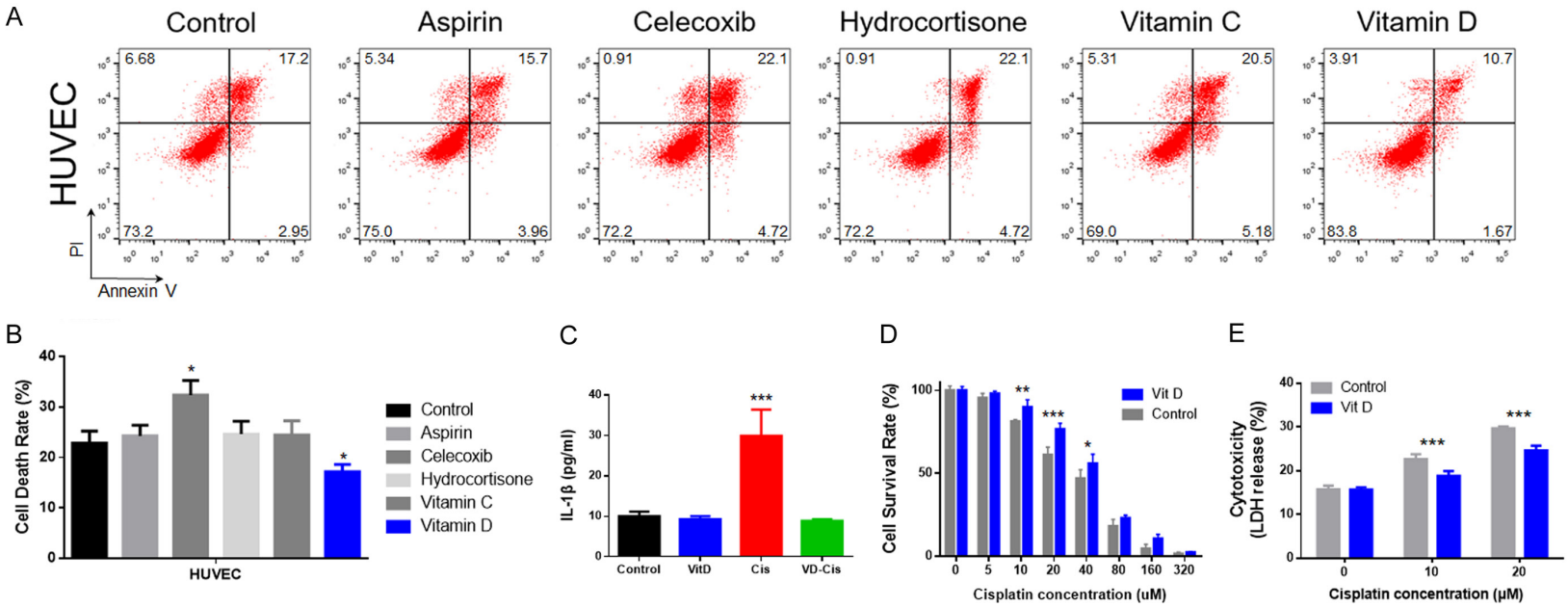

Figure S6. (A) FCM revealed cisplatin-induced cell death in HUVECs after pre-treatment with aspirin, celecoxib, hydrocortisone, vitamin C and vitamin D; (B) Statistical analysis of the cell death rates shown in (A); (C) ELISA revealed reduced IL-1β secretion in HUVECs pre-treated with vitamin D; (D) Gradient concentration of cisplatin-treated HUVECs pre-treated with vitamin D, which increased cisplatin tolerance; (E) Cytotoxicity assay revealed that LDH release was reduced in HUVECs pre-treated with vitamin D compared with control cells after cisplatin treatment. (cisplatin treatment: 40 μM, 24 hours for B-D).